CALIBRATION OF POTENTIAL FIELD FUNCTIONS OF THE POTENTIAL FIELD THEORY BASED MODEL OF DRIVER BEHAVIOR

A Thesis Submitted
in Partial Fulfillment of the Requirements
for the Degree of
M.Tech

by

Ashish Mahajan

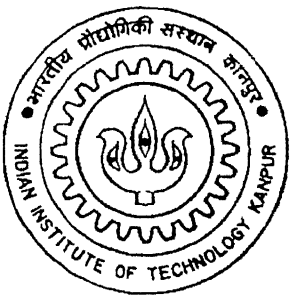

to the

DEPARTMENT OF CIVIL ENGINEERING
INDIAN INSTITUTE OF TECHNOLOGY KANPUR

October, 2000

CERTIFICATE

This is to certify that this M.Tech thesis work entitled **CALIBRATION OF POTENTIAL FIELD FUNCTIONS OF THE POTENTIAL FIELD THEORY BASED MODEL OF DRIVER BEHAVIOR** *has been carried out by* **Ashish Mahajan** *under my supervision and it has not been submitted elsewhere for a degree.*

October 30 ,2000

Dr. Partha Chakroborty, Ph.D.
Assistant Professor
Dept. of Civil Engg.
Indian Institute of Technology
Kanpur

ACKNOWLEDGEMENTS

It gives me immense pleasure to express my deep sense of gratitude to my thesis supervisor, Dr. Partha Chakroborty for his instruction, criticism, suggestions and encouragement throughout the course of my study and providing me a peaceful lab with good computation facilities. I can not forget the way he encouraged and trained me to think about the problem in hand by spending his precious time siting with me. His help in arranging thesis in final stage is highly appreciated.

I would like to thank Dr. B. R. Marwah, and Dr. S. P. Palaniswamy for their help and useful lecture during my course work.

I thank all my friend circle saurabh, tathagat, sajit saheb, praveen, lalit, neelima, sushovan, anjan and nayak, sudhir, vyas, munni, and nem who give me a good company and made my stay at IIT Kanpur most memorable.

The blessing of my parents, sisters Smt. pratibha and ku. manisha helped me throughout my thesis work. Their love, affection and care has always helped me to pass hurdles of life without any pain. I will remain indebted to them throughout my life.

Ashish Mahajan

DEDICATION

To my parents

Shri. B. K. Mahajan and Smt. Usha Mahajan

Contents

List of Figures

List of Tables

ABSTRACT

In recent time a single comprehensive model for driver behavior has been developed using potential field theory of the robot motion planning. These models, at present, do not have any mechanism for calibrating their parameters. In this thesis an attempt is made to develop a mechanism which can be used to calibrate the parameters of these models. Results using the proposed mechanism show that the proposed mechanism can form the ground work for the a larger and more extensive calibration mechanism for the potential field theory based model of driver behavior.

Chapter 1

INTRODUCTION

Microscopic models of traffic flow form the foundation for the theory of traffic flow. Microscopic models attempt to predict the drivers behavior in small interval of time. Driver behavior is captured in these models through to variables: (i) the steering angle chosen by driver, and (ii) the acceleration/deceleration rate use by the driver. Although, various microscopic models exist (Pipes [4], Forbes [5, 6], Chandler et al. [7], Herman et al. [8, 9], Gazis et al. [10, 11], Rockwell et al. [12], May and Killer [13], Kikuchi and Chakroborty [14], Chakroborty and Kikuchi [15], Taragin [16], Michaels and Gozan [17]) only two of them, namely, Vasishta [2] and Agrawal [1] attempt at developing a comprehensive model of driver behavior. That is, unlike the others, these models attempt to capture driver behavior in various driving situations (like, car-following, overtaking, free flow, etc) through a single model. These models are based on the potential field theory of robot motion planning (see Latombe [3]). However Vasishta [2] and Agrawal [1] do not suggest how various parameters of their model can be calibrated given data on observed driver behavior. This thesis attempts to overcome this short coming by developing a calibration algorithm.

The thesis is divided into six chapters of which this is the first. The second chapter describes the problem tackled here and lays down the scope of present thesis. The third chapter presents results from a detail parametric study of the potential field theory based models. The fourth chapter describes the proposed calibration mechanism. The fifth chapter presents the results obtained using proposed calibration mechanism for various different scenarios. The sixth and last chapter concludes this thesis by summarizing the achievement of this thesis and by discussing the short comings of the present work.

Chapter 2

PROBLEM STATEMENT AND SCOPE OF STUDY

In this thesis the problem of calibrating the parameters of potential field functions of potential field based theory model of traffic flow is studied. However, before presenting a detail description of problem and scope of study, a brief description of potential field theory based model of traffic flow is given.

2.1 Potential field theory based model

Vasishta [2] and Agrawal [1] have over last three years developed the potential field theory based model of traffic flow. This is a microscopic model which basically describe drivers' action in terms of steering angle choice and acceleration/deceleration choice under different driving scenarios. In this models a driving scenarios is defined as a conglomeration of traffic and roadway features in the immediate vicinity of a driver. Roadway feature, like road edges, curvature, potholes, etc, and traffic features, like parked vehicles, moving vehicles in the same and opposite direction, are all assumed to be obstacles which a driver avoid while driving. Each of these obstacle are assumed to emanate a repulsive force field around it. This force field is referred to as a potential field and is described mathematically through a potential field function.

The predicted actions of a driver, from this model, depends largely on the potential field functions of the obstacles. Despite this depends no attempt are made either by Vasistha [2] and

Agrawal [1] to develop the mechanism for calibrating the parameters of these functions. This lack of an available mechanism formed the motivation for this study.

2.2 Problem statement and scope of study

The problem here, as stated earlier is to develop a mechanism which can be used to calibrate the parameter of potential field functions. The mechanism should take as input the observed path of a driver in a real world situation and the predicted path from the model for the same situation with an initial assumed parameter values. The mechanism should produce as its output a set of calibrated parameter values which when used by the model produces the predicted path similar to the observed path.

In order to develop such a mechanism two tasks need to be accomplished. First, a study on the effect of different parameters on the predicted path need to be conducted. Second, based on the information available from this study, rules of calibration which tell us how to change the parameter values need to be developed. These tasks formed the subject matter of next two chapters.

Given the complex nature of potential field functions and the complex manner in which they affect the predicted path the scope of this study is kept limited. Basically in this study the scope is limited to calibrating the parameters of road edges and static obstacles likes potholes, parked vehicles, etc.

Chapter 3

PARAMETRIC STUDY OF POTENTIAL FUNCTIONS

As stated earlier, the tasks to be undertaken in this thesis are (i) to study the effect of potential field function parameter values on the driver's position profile and (ii) to develop an algorithms for modifying these parameters so that the predicted path emulates the observed path better. The first of these two tasks is the subject of this chapter. The chapter is divided into three sections. The first presents the potential field function for the obstacles (or driving features) which are considered in this thesis. The second and third sections present the effect of the parameters of the potential field functions.

3.1 Potential field functions for the different driving features

The driving features (i.e. roadway or traffic features) considered in this thesis are: (i) road edges and (ii) static obstacle (like potholes, parked vehicle etc). In this section the potential field function for these features as used by Vasishta [2] are presented. This is done so as to make the description of the parametric study complete.

3.1.1 Potential field function for road edges

The potential field function for a road edge is given by

$$U_e = ae^{-bz} \tag{3.1}$$

where, z is the distance from the road edge, a is a parameter which denotes the potential at the edge and b is a parameter which determines the rate of decrease of the potential with z. Specifically the function for the left edge, U_{LE}, and the right edge, U_{RE}, can be written as

$$U_{LE} = a_1 e^{-b_1 x} \tag{3.2}$$

and

$$U_{RE} = a_2 e^{-b_2(w-x)} \tag{3.3}$$

where, x is the distance from the left edge of the road; a_1 and a_2 are the potential values at the left edge and right edge respectively; b_1 and b_2 are the slope parameters for the left edge and right edge potential field functions respectively. The combined potential due to both the edges of the road, U_{be}, can be written as

$$U_{be} = a_1 e^{-b_1 x} + a_2 e^{-b_2(w-x)} \tag{3.4}$$

Note that it is meaningful to only work at U_{be} rather then then U_{RE} and U_{LE} since a road always has two edges. Further as suggested by Vasishta [2]

- $b_1 > 0$, $b_2 > 0$
- $a_2 > a_1$ (because, in India drivers follow a "keep left" policy)

3.1.2 Potential field function for static obstacles

The potential field function for a static obstacle is given by

$$U_o = a_4 e^{-f(y)[(\frac{x-x_0}{m_i})^2 + (\frac{y-y_0}{m_a})^2 - 1]\rho} \tag{3.5}$$

where

$$\rho = \begin{cases} 1 & \text{if } (\frac{x-x_0}{m_i})^2 + (\frac{y-y_0}{m_a})^2 \geq 1 \\ 0 & \text{otherwise} \end{cases}$$

and

$$f(y) = \begin{cases} b_4 & \text{if } y \leq t_1 \\ \alpha y^3 + \beta y^2 + \gamma y + \delta & \text{if } t_1 < y < t_2 \\ b_5 & \text{if } y \geq t_2 \end{cases}$$

where (x, y) is the coordinate of any point on the road, (x_0, y_0) are the coordinates of the center of the obstacle; m_i, m_a are respectively the semi-minor and the semi-major axes of the ellipse which circumscribes the obstacle; ρ is a boolean variable representing whether point (x, y) is inside the ellipse ($\rho = 0$) or not ($\rho = 1$). Further, a_4 is the maximum value U_o can take and $f(y)$ is a function which determines the slope for U_o. t_1 and t_2 are lower and upper limits of y with which $f(y)$ varies.

Before leaving this section clarifications regarding (i) the determination of the coefficients of $f(y)$ and (ii) m_i need to be given.

Clarification (i)

Given the value of b_4, b_5 and t_1, t_2 the coefficients $\alpha, \beta, \gamma, \delta$ are calculated using the following restrictions: (i) $f(y)$ should pass through (t_1, b_4) and (t_2, b_5), and (ii) $f(y)$ should pass through a point *tp* where its slope is also zero. Therefore, it needs to noted that *tp* is also a parameter which affects the predicted path.

Clarification (ii)

The parameter m_i is not considered as a calibration parameter, since Vasishta [2] suggests a procedure for selection of m_i from the size and shape of a obstacle. Hence given the obstacle, m_i is fixed.

3.2 Effect of parameters of U_{be} on the predicted driver path

The following are identified, as indicated by Vasishta [2], as parameters of U_{be}: a_1, a_2, b_1 or b_2 and $\frac{b_1}{b_2}$. The effect of these parameters on the predicted path are studied here.

Effect of a_1

Figure 3.1 shows the effect of a_1 on predicted driver path on a 6 m road keeping all other parameters as constant ($a_2 = 4.0$, $b_1 = 0.32641$, $b_2 = 0.04663$ and $\frac{b_1}{b_2} = 7.0$). It can be seen that, when the value of a_1 increases the predicted path shifts towards right edge of the road. The same behavior can be observed from other road widths also.

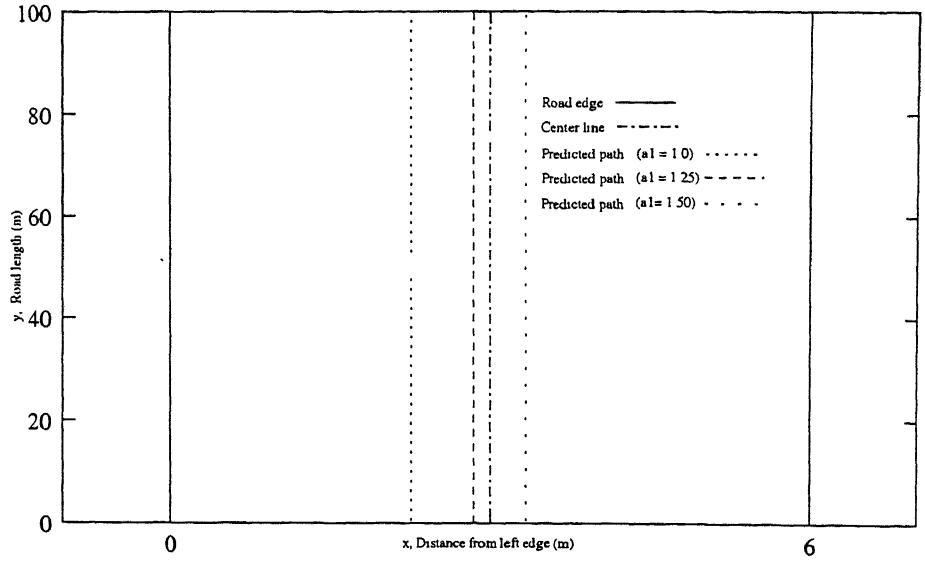

Figure 3.1: Effect of a_1

Effect of a_2

Figure 3.2 shows the effect of a_2 on predicted driver path on a 6 m road keeping all other parameters as constant ($a_1 = 1.0$, $b_1 = 0.32641$, $b_2 = 0.04663$ and $\frac{b_1}{b_2} = 7.0$). It can be seen that, when the value of a_2 increases path shifts towards left edge of the road. The same behavior can be observed from other road widths also.

Effect of b_1 or b_2

Figure 3.3 shows the effect of b_2 on driver path on a 6 m road keeping ratio of $\frac{b_1}{b_2}$ and all other parameters as constant ($a_1 = 1.0$, $a_2 = 4.0$ and $\frac{b_1}{b_2} = 7.0$). It can be seen that, when the value of b_2 increases the predicted path shifts towards left edge of the road. It should be noted that keeping $\frac{b_1}{b_2}$ constant and changing b_2 also implies changing b_1 in the same direction (i.e. increasing b_2 implies increasing b_1). Similar behavior can be observed for different road widths and $\frac{b_1}{b_2}$ ratio.

Effect of $\frac{b_1}{b_2}$

The effect of this can not be studied separately from effect of b_1 or b_2 because changing $\frac{b_1}{b_2}$ implies a change in b_1 or b_2. Hence no clear direction in the shift of the predicted path can be observed by changing $\frac{b_1}{b_2}$. Hence no result is presented here. As will be seen later, knowledge of the effect of $\frac{b_1}{b_2}$ is not crucial to development of the calibration algorithms– the primary purpose of the thesis.

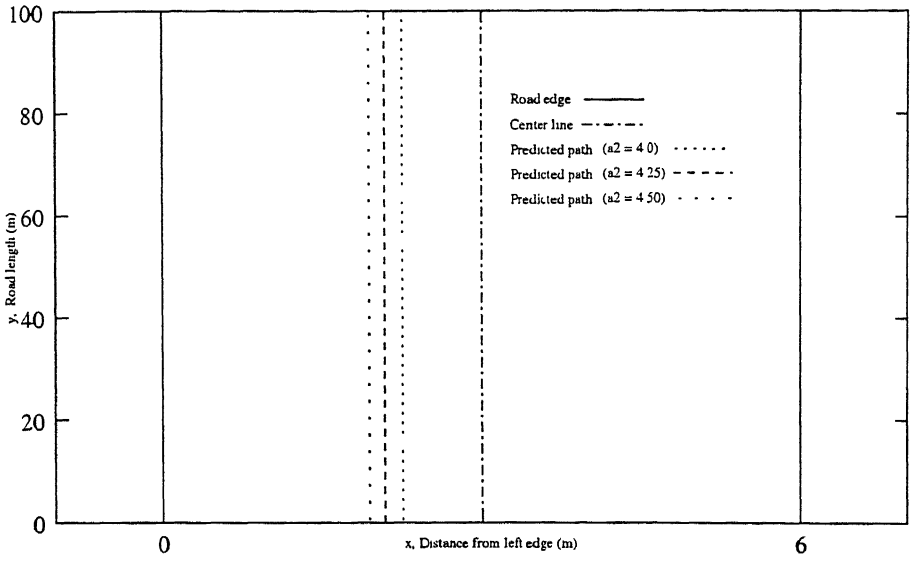

Figure 3.2: Effect of a_2

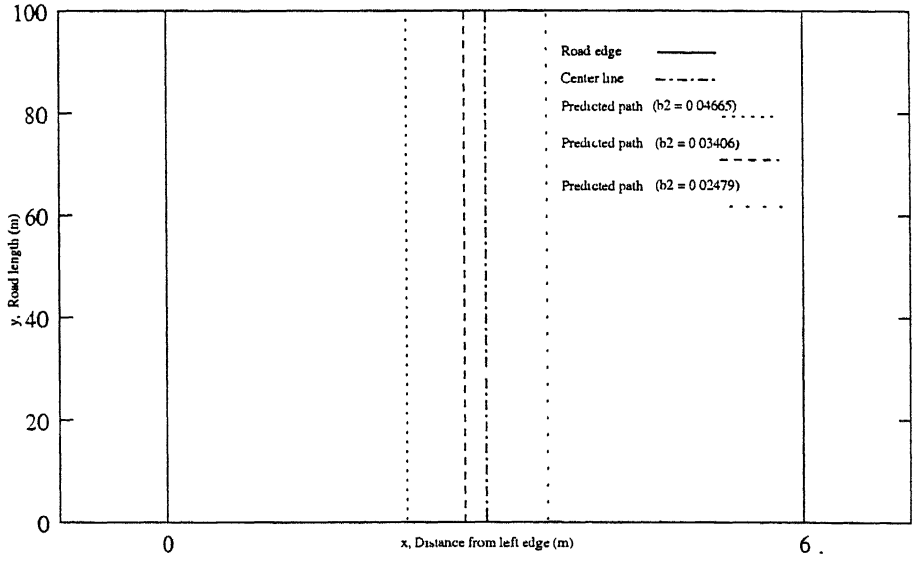

Figure 3.3: Effect of b_2

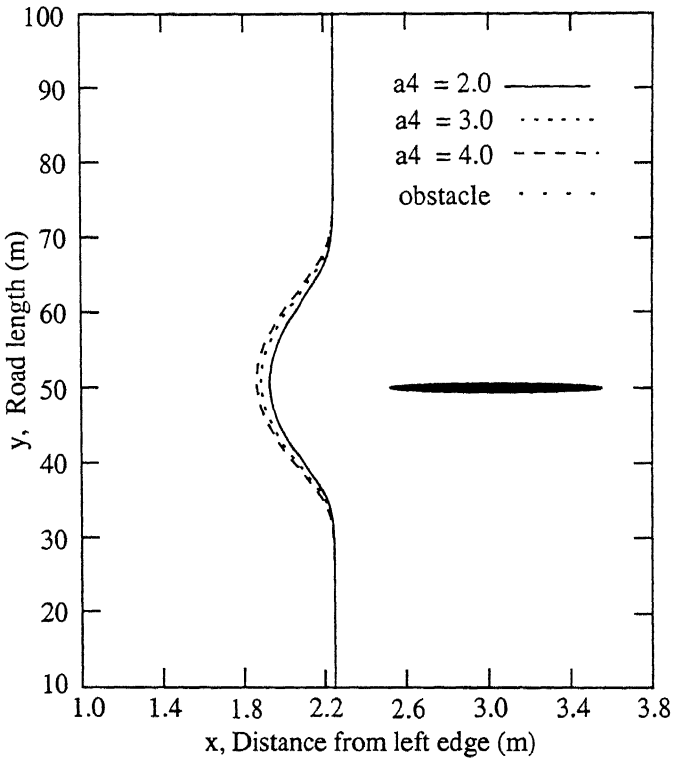

Figure 3.4: Effect of a_4

3.3 Effect of parameters of U_o on predicted driver path

The following are identified as parameters of U_o: a_4, m_a, b_4, b_5, tp, t_1, and t_2. The effect of these parameters on the predicted path are studied here.

Effect of a_4

Figure 3.4 shows the effect of a_4 on the predicted driver path on a 6 m road keeping all other parameters as constant. The value of the other parameters for the predicted paths in Figure 3.4 are: (i) edge potential function parameters, $a_1 = 1.0$, $a_2 = 4.0$, $b_1 = 0.32641$, $b_2 = 0.04663$ and (ii) obstacle potential function parameters, $m_i = 0.5$, $m_a = 9.0$, $b_4 = 2.0$, $b_5 = 2.0$, $\alpha = 0$, $\beta = 0$, $\gamma = 0$, $\delta = 2.0$, $t_1 = 20$, $t_2 = 80$ and $tp = (2, 50)$. It can be seen that when a_4 increases the deviation in the transverse direction (i.e. direction along the width) as well as deviation in the longitudinal direction (i.e. direction along the length) increase. Further, the effect is symmetrical about a transverse axis thought the center of the obstacle. Also note that effect in the longitudinal direction is lesser than in the transverse direction.

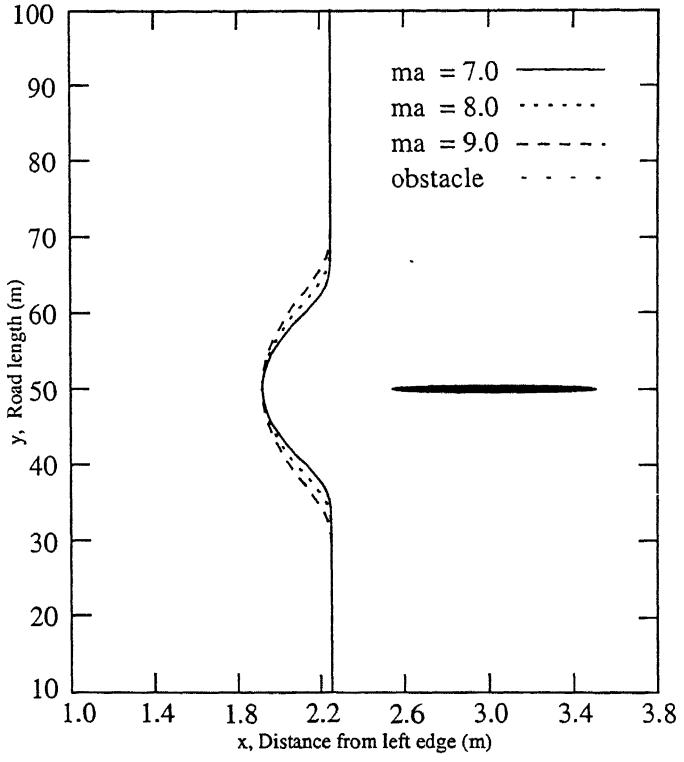

Figure 3.5: Effect of m_a

Effect of m_a

Figure 3.5 shows the effect of m_a on the predicted driver path on a 6 m road keeping all other parameters as constant. The values of the other parameters for the predicted paths in Figure 3.5 are: (i) edge potential function parameters, $a_1 = 1.0$, $a_2 = 4.0$, $b_1 = 0.32641$, $b_2 = 0.04663$ and (ii) obstacle potential parameters, $a_4 = 4.0$ $m_i = 0.5$, $b_4 = 2.0$, $b_5 = 2.0$, $\alpha = 0, \beta = 0, \gamma = 0, \delta = 2$, $t_1 = 20$, $t_2 = 80$ and $tp = (2, 50)$. It can been seen that, when m_a increases the transverse deviation (along the width of road) as well as deviation in the longitudinal (i.e. direction along the length) increase. However, the effect in longitudinal direction pronounced then in lateral direction; in fact, the maximum transverse deviation is insensitive to m_a value. Further, the deviations are symmetric about a transverse axis through the center of the obstacle.

Effect of b_4

Figure 3.6 shows the effect of b_4 on a 6 m road keeping all other parameters as constant. The values of the other parameters for the predicted paths in Figure 3.6 are: (i) edge potential function

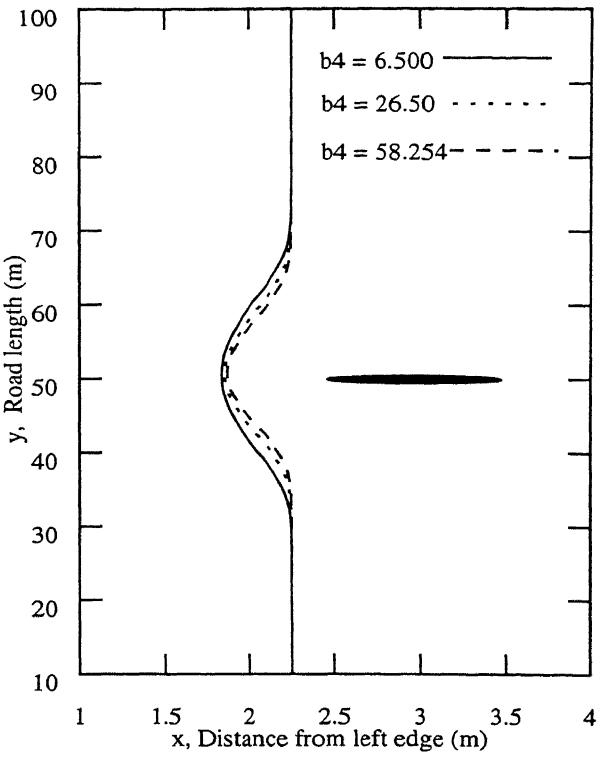

Figure 3.6: Effect of b_4

parameters, $a_1 = 1.0$, $a_2 = 4.0$, $b_1 = 0.032641$, $b_2 = 0.04663$ and (ii) obstacle potential function parameters, $a_4 = 2.0$, $m_i = 0.5$, $m_a = 8.0$, $t_1 = 10.0$, $b_5 = 2.5$, $t_2 = 80.0$ and $tp = (50, 1.5)$. It can be seen that, when the value of b_4 increases the transverse and longitudinal deviation on both side of tp decrease. The decrease, is however least at $y = 50$, the abscissa value for tp.

Effect of b_5

Figure 3.7 shows the effect of b_5 on 6 m a road keeping all other parameters as constant. The values of the other parameters for the predicted paths in Figure 3.7 are: (i) edge potential function parameters, $a_1 = 1.0$, $a_2 = 4.0$, $b_1 = 0.032641$, $b_2 = 0.04663$ and (ii) obstacle potential function parameters, $a_4 = 2.0$, $m_i = 0.5$, $m_a = 8.0$, $b_4 = 2.50$, $t_1 = 20$, $t_2 = 75$ and $tp = (50, 1.5)$ It can be seen that, when b_5 increases transverse and longitudinal deviation on both side of tp decrease. The decrease, is however least at $y = 50$, the abscissa value for tp.

Effect of tp

In order to study the effect of tp six cases are constructed. These are described in following table

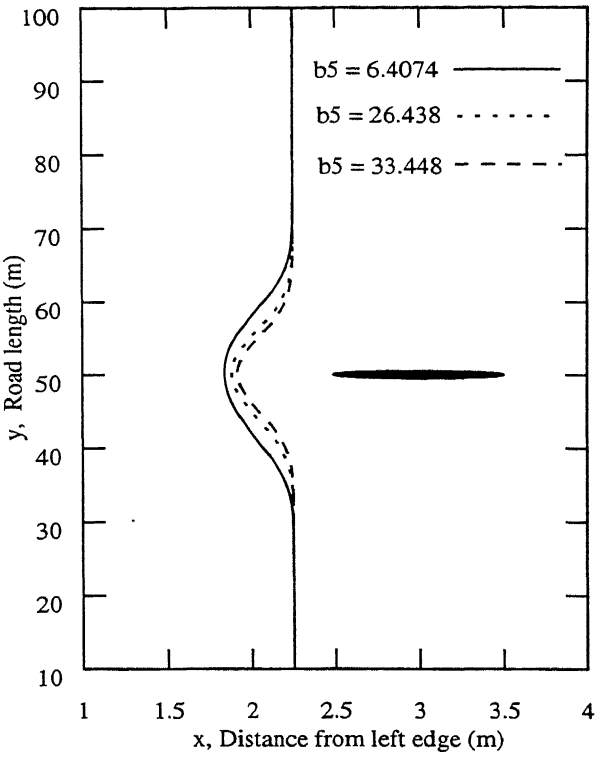

Figure 3.7: Effect of b_5

Table 3.1: Cases for studying *tp*

abscissa of tp	*ordinate of tp*		
	below b_4 *and* b_5	*above* b_4 *and* b_5	*in between* b_4 *and* b_5
above the y coordinate of obstacle	Case I	Case III	Case V
below the y coordinate of obstacle	Case II	Case IV	Case VI

The specific details of the cases and their corresponding figures are given below.

Cases I and II

Figure 3.8 shows five paths, each for a different value of the abscissa of *tp*. The obstacle is at (3, 50), hence, two of the paths are for values which place the *tp* above the y coordinate of obstacle (case I), two of the paths are for values which place the *tp* below the y coordinate of obstacle (case II), and one path is when the *tp's* abscissa value equal to the y coordinate of the obstacle. All the paths are plotted for the following parameter values: (i) edge potential function parameters, $a_1 = 1.0$, $a_2 = 4.0$, $b_1 = 0.032641$, $b_2 = 0.04663$ and (ii) obstacle potential function parameters, $a_4 = 2.0$, $m_i =$

0.5, $m_a = 8.5$, $b_4 = 3.00$, $t_1 = 0.0$, $b_5 = 3.0$, $t_2 = 100.0$. It can be seen from figure that as tp moves away from the y coordinate of obstacle. The deviation reduce, irrespective of whether tp is above or below the position of the obstacle.

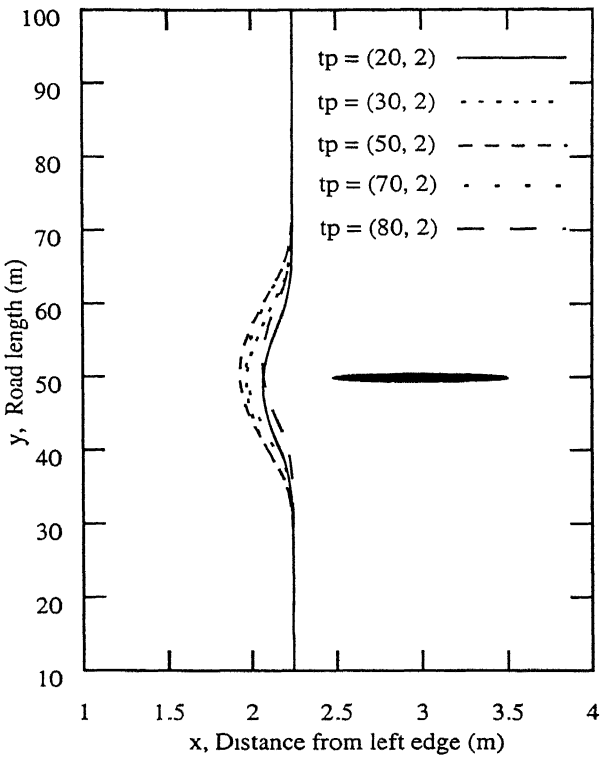

Figure 3.8: Effect of tp in Cases I and II

Cases III and IV

Figure 3.9 shows the five paths, each for a different value of the abscissa of tp. The obstacle is at (3, 50), hence, two of the paths are for values which place the tp above the y coordinate of obstacle (Case III), two of the paths are for values which place the tp below the y coordinate of obstacle (case IV) and one path is when the $tp's$ abscissa value equal to the y coordinate of the obstacle. All the paths are plotted for the following parameter values: (i) edge potential function parameters, $a_1 = 1.0$, $a_2 = 4.0$, $b_1 = 0.032641$, $b_2 = 0.04663$ and (ii) obstacle potential function parameters, $a_4 = 2.0$, $m_i = 0.5$, $m_a = 8.5$, $b_4 = 3.00$, $t_1 = 0.0$, $b_5 = 3.0$, $t_2 = 100.0$. It can be seen from figure that as tp moves away from the y coordinate of obstacle. The deviation increase, irrespective of whether tp is above or below the position of the obstacle.

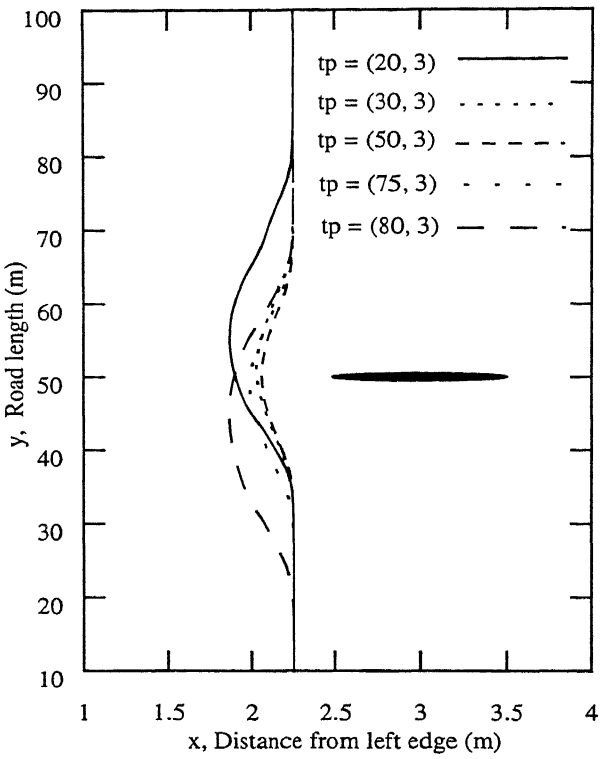

Figure 3.9: Effect of tp in Cases III and IV

Cases V and VI

In these Cases, the ordinate of tp is in between b_4 and b_5. For the same reasons as above five paths are plotted and shown in Figure 3.10. Each of these paths are plotted for the following parameter values: (i) edge potential function parameters, $a_1 = 1.0$, $a_2 = 4.0$, $b_1 = 0.32641$, $b_2 = 0.04663$ and (ii) obstacle potential parameters, $a_4 = 2.0$, $m_i = 0.5$, $m_a = 8.5$, $b_4 = 3.50$, $t_1 = 0.0$, $b_5 = 1.5$, $t_2 = 100.0$. It can be observed from the Figure 3.10 that if the obstacle of tp is on the same side of the obstacle as the lesser of b_4 and b_5 (in this case $b_4 < b_5$) [notice here that b_4 is the slope on the upstream side of obstacle and b_5 is the slope on the downstream side of obstacle] then as tp moves away from obstacle the deviations increase. If, however tp is on the same side of obstacle as the greater of b_4 and b_5 (in this case b_5) then as tp moves away from the obstacle the deviations decrease.

Another aspect, which needs to be pointed out here is the effect of only changing the ordinate of tp keeping all other parameters fixed. Figure 3.11 shows four paths. Each is drawn for a different value of the ordinate. As can be seen, from the figure, the deviation decrease as the ordinate value

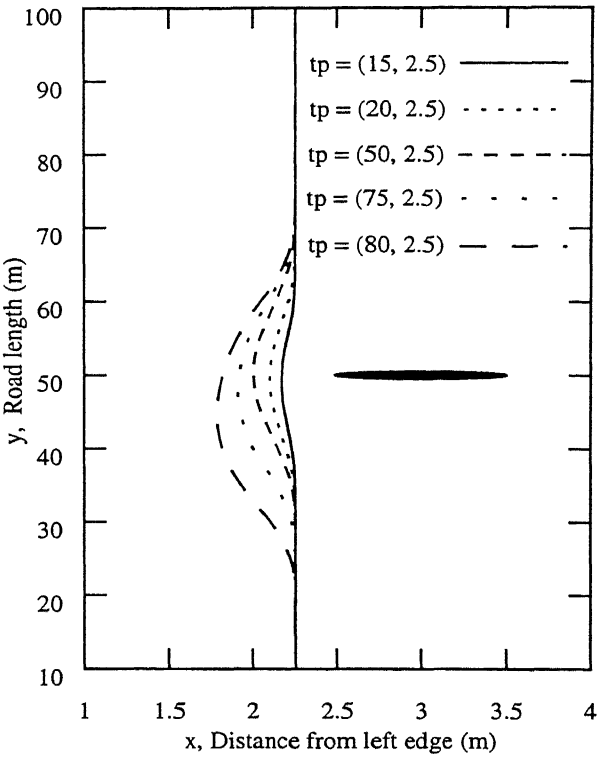

Figure 3.10: Effect of *tp* in Cases V and VI

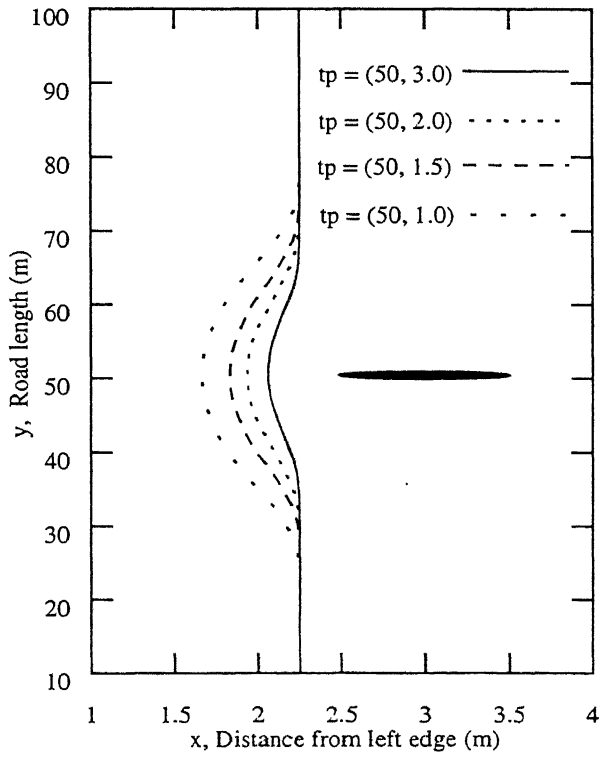

Figure 3.11: Effect of ordinate of *tp*

increases, irrespective of whether they are greater or smaller than b_4 and b_5.

Effect of t_1

Figure 3.12 shows the effect of t_1 on the predicted path of driver on a 6 m road keeping all other parameters as constant. The values of the other parameters for the predicted paths in Figure 3.12 are: (i) edge potential function parameters, $a_1 = 1.0$, $a_2 = 4.0$, $b_1 = 0.32641$, $b_2 = 0.04663$ and (ii) obstacle potential parameters, $a_4 = 2.0$, $m_i = 0.5$, $m_a = 8.5$, $b_4 = 1.9$, $b_5 = 1.9$, $t_2 = 85.0$ and $tp = (50, 3)$. It can be seen that, when t_1 moves away from the obstacle lateral and longitudinal deviations in the paths increase, although minimally.

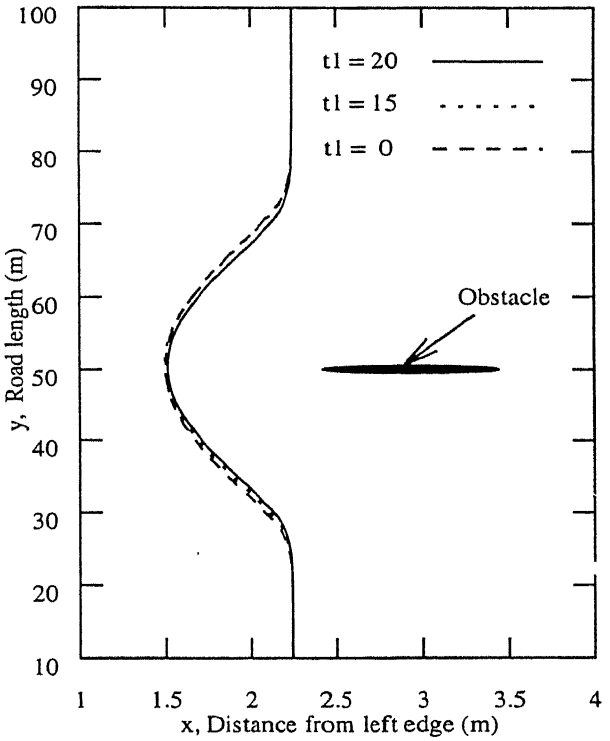

Figure 3.12: Effect of t_1

Effect of t_2

Figure 3.13 shows the effect of t_2 on the predicted path of driver on a 6 m road keeping all other parameter as constant. The values of the other parameters for the predicted paths in Figure 3.13 are: (i) edge potential function parameters, $a_1 = 1.0$, $a_2 = 4.0$, $b_1 = 0.32641$, $b_2 = 0.04663$ and (ii) obstacle potential parameters, $a_4 = 2.0$, $m_i = 0.5$, $m_a = 8.5$, $b_4 = 1.90$, $t_1 = 0.0$, $b_5 = 1.9$ and

$tp = (50, 3)$. It can be seen that, when t_2 moves away from the obstacle deviations in the paths increase, although minimally.

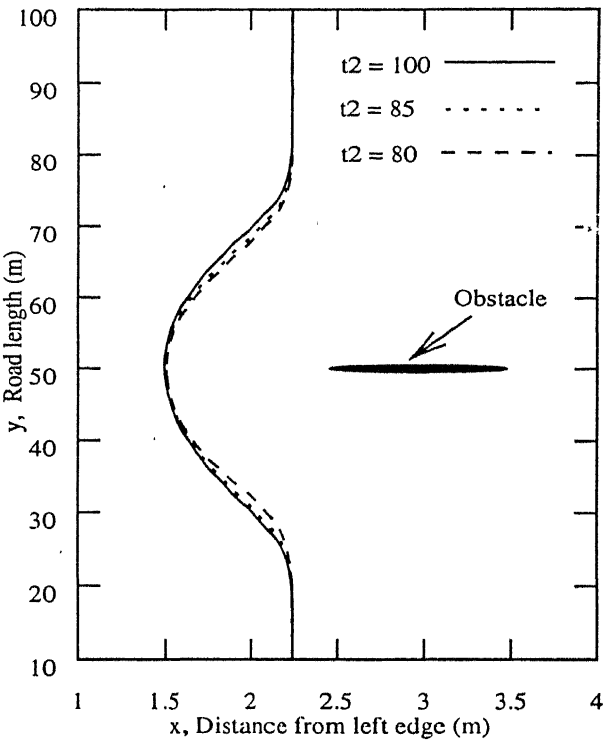

Figure 3.13: Effect of t_2

Based on the above parametric study, few important points relevant to the calibration process emerge.

1. The parameters of the potential functions changes the predicted path in a variety of ways. Thus, it is felt that one can modify an initially predicted path to the observed path by varying these parameters.

2. Further, it is possible to determine a direction of change of certain parameters given the observed and initially predicted path. For example, if the observed path lies to the left of the initially predicted path one can find that a_1 has to be decrease, a_2 has to be increase etc.

3. There are however certain parameters for which it is not possible to predict any such direction of change.

4. Lastly, one could identify certain parameters such as, t_1 and t_2, which do not affect the predicted path much.

Chapter 4

PROPOSED CALIBRATION PROCESS

In this chapter the proposed procedure for calibration are described. The chapter is divided into three sections in the first section overview of the proposed calibration procedure is explained. Section two describes Stage I of calibration procedure. Section three describes Stage II of calibration procedure.

4.1 Overview of the proposed calibration procedure

Given the observed path and the initial path (obtained using an initial set of values for the parameters of the potential field theory model) the calibration procedure uses the following steps to calibrate the parameter values of the potential field functions.

1. Plot the initial path and observed path on a Cartesian space with abscissa, x, as the distance from the left edge of the road and ordinate, y, as the distance along the road from some arbitrary location.

2. Divide the length of the road into a number of cross-sections (i.e. section with same ordinate). The cross sections can be arbitrarily close.

3. For a cross section i, determine the error E_i as follows:

$$E_i = |(X^i_{obs} - X^i_{in})| \tag{4.1}$$

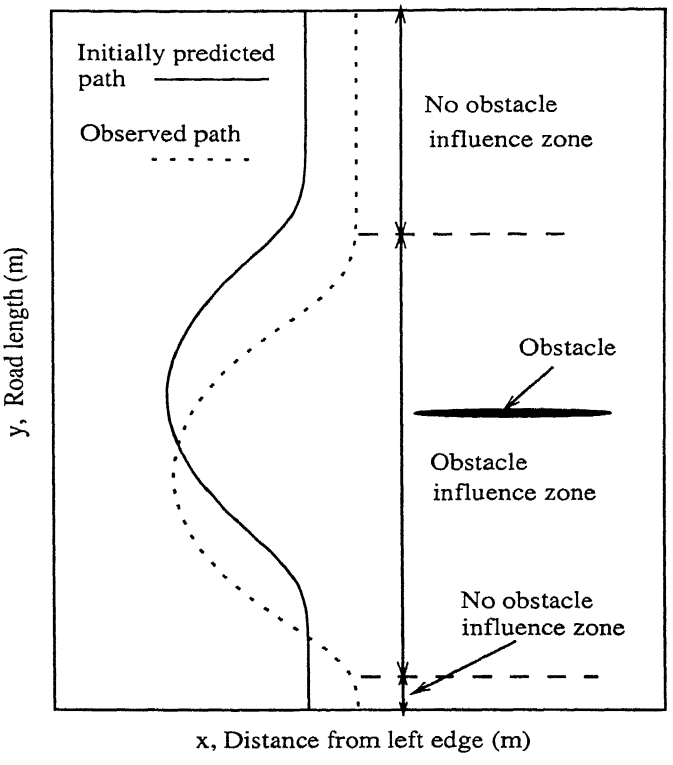

Figure 4.1: Stretch of the road illustrating the initially predicted path and the observed path

where E_i is the absolute error at i^{th} cross-section of the road, X^i_{obs} and X^i_{in} are the abscissa of observed and initial paths respectively at the i^{th} cross-section.

4. Check whether the E_i at each cross-section is less than some threshold limit; if not, then correction in parameters of potential functions are required so go to next step; if yes, stop the process.

5. Determine E_i in the no-obstacle influence zone (see the Figure 4.1 for the definition of no-obstacle influence zone).

6. Check whether the E_i in the no-obstacle influence zone is less than the threshold limit; if no, apply Stage I of calibration procedure (as explained in Section 4.2); if yes, determine the characteristics of the observed path relative to the initial path after Stage I of calibration (as explained in Section 4.3) and apply Stage II correction rules to modify the parameter values of obstacle potential field function (as explained in Section 4.3.2).

7. Replot initial path with modified (corrected) parameters of the potential functions and go to Step 2. These steps are shown schematically in Figure 4.2.

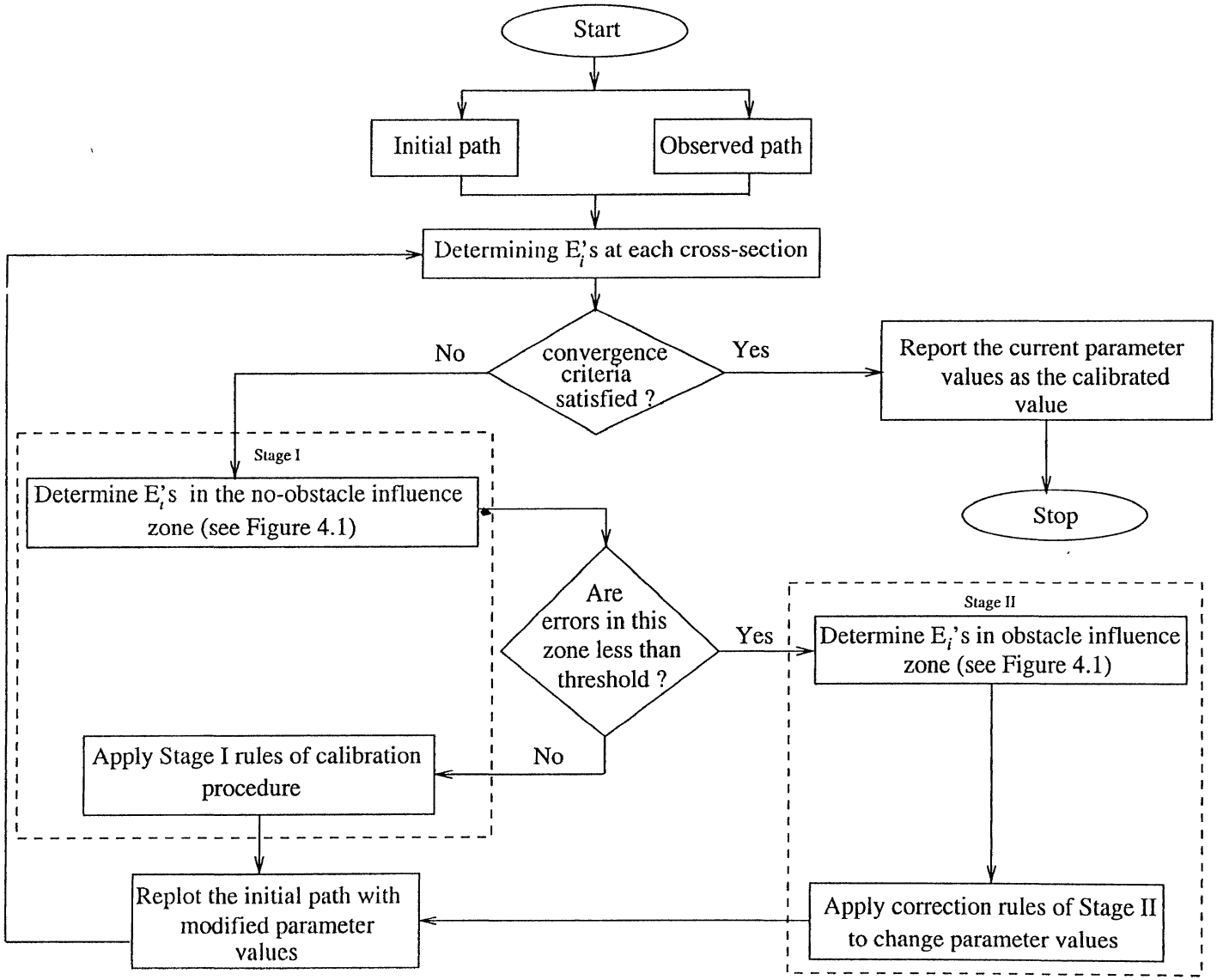

Figure 4.2: Overview of the proposed calibration procedure

4.2 Calibration procedure for Stage I

In Stage I, the corrections are applied to the parameters of the road edge potential functions to remove the errors in the no-obstacle influence zone (see the Figure 4.1 for the definition of no-obstacle influence zone) since in this zone only edge potential functions are active. The algorithm for Stage I corrections is based on the study performed in Chapter 3 on the effect of different parameters on the predicted path. As can be seen, from the study varying different parameters do have similar effects on the predicted path. For example, the predicted path shifts towards the right edge if a_1 is increased or a_2 is decreased, etc. Also, it can be observed that the rate of change of the predicted path with respect to different are different. Based on these observation, the algorithm is formulated thus:

1. Determine X^i_{obs} and X^i_{in} at i^{th} cross-section of road in no-obstacle influence zone.
2. Determine absolute error at i^{th} cross-section in no-obstacle influence zone, E_i, as given below.

$$E_i = |(X^i_{obs} - X^i_{in})| \tag{4.2}$$

3. Check whether E_i is less than threshold, if no, the correction in edge potential field function is required so go to next step; if yes, no correction is required so stop the process.
4. If $X^i_{obs} > X^i_{in}$ increase a_1 and decrease a_2 (or if $X^i_{obs} < X^i_{in}$ decrease a_1 and increase a_2) with small step size without violating the following condition: $a_2 > a_1$; and $a_2 e^{-b_2 w} + a_1 < a_1 e^{-b_1 w} + a_2$).
5. Either increase or decrease the value of b_2 with small step size (keeping in mind the conditions: $a_2 > a_1$; and $a_2 e^{-b_2 w} + a_1 < a_1 e^{-b_1 w} + a_2$) so that error calculated by Equation 4.2 is further reduced and check whether error is less than threshold limit if yes, stop the procedure; if not, go to next step. Here, both increase and decrease of b_2 is tried because the position of the path also depends on $\frac{b_1}{b_2}$ and as such a clear understanding of the effect of b_2 alone is not available.
6. Either increase or decrease the value of b_1 (keeping in mind the conditions: $a_2 > a_1$; and $a_2 e^{-b_2 w} + a_1 < a_1 e^{-b_1 w} + a_2$) with small step size so that error calculated by Equation 4.2 further reduce and check whether it is less than threshold limit if not, go to Step 4. Here, both increase and decrease of b_1 is tried because the position of the path also depends on $\frac{b_1}{b_2}$ and as such a clear understanding of the effect of b_1 alone is not available.

After applying Stage I corrections, in theory, the predicted path and the observed path in the no obstacle influence zone should become indistinguishable. Figure 4.3 shows a schematic of how the predicted would be in comparison to the observed path before and after Stage I calibrations.

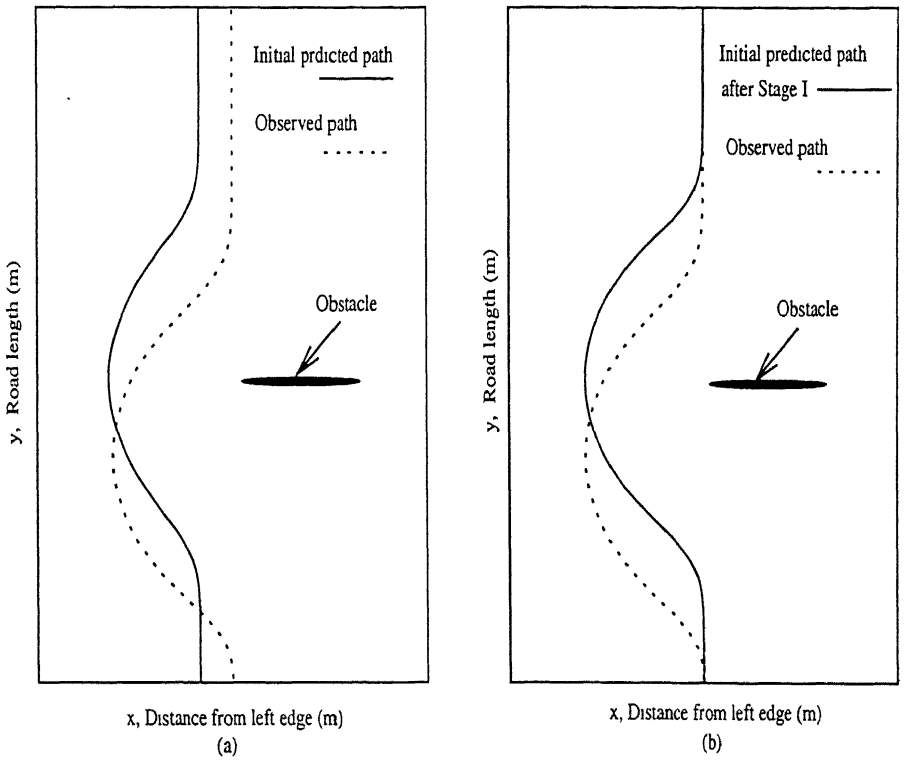

Figure 4.3: (a) Comparison of predicted path and observed path (a) before Stage I calibration and (b) after Stage I Calibration

4.3 Calibration procedure for Stage II

In stage two, corrections are applied to the parameters of obstacle potential field function. The calibration procedure can be divided into two parts:

1. Measurement of characteristics of predicted path relative to observed path in obstacle influence zone after the completion of Stage I calibrations.

2. Application of the rules of correction developed here to the parameters of the obstacle potential field function.

4.3.1 Measurement of characteristics of predicted path after Stage I relative to observed path.

The characteristics of the predicted path are measured in terms of the following factors:

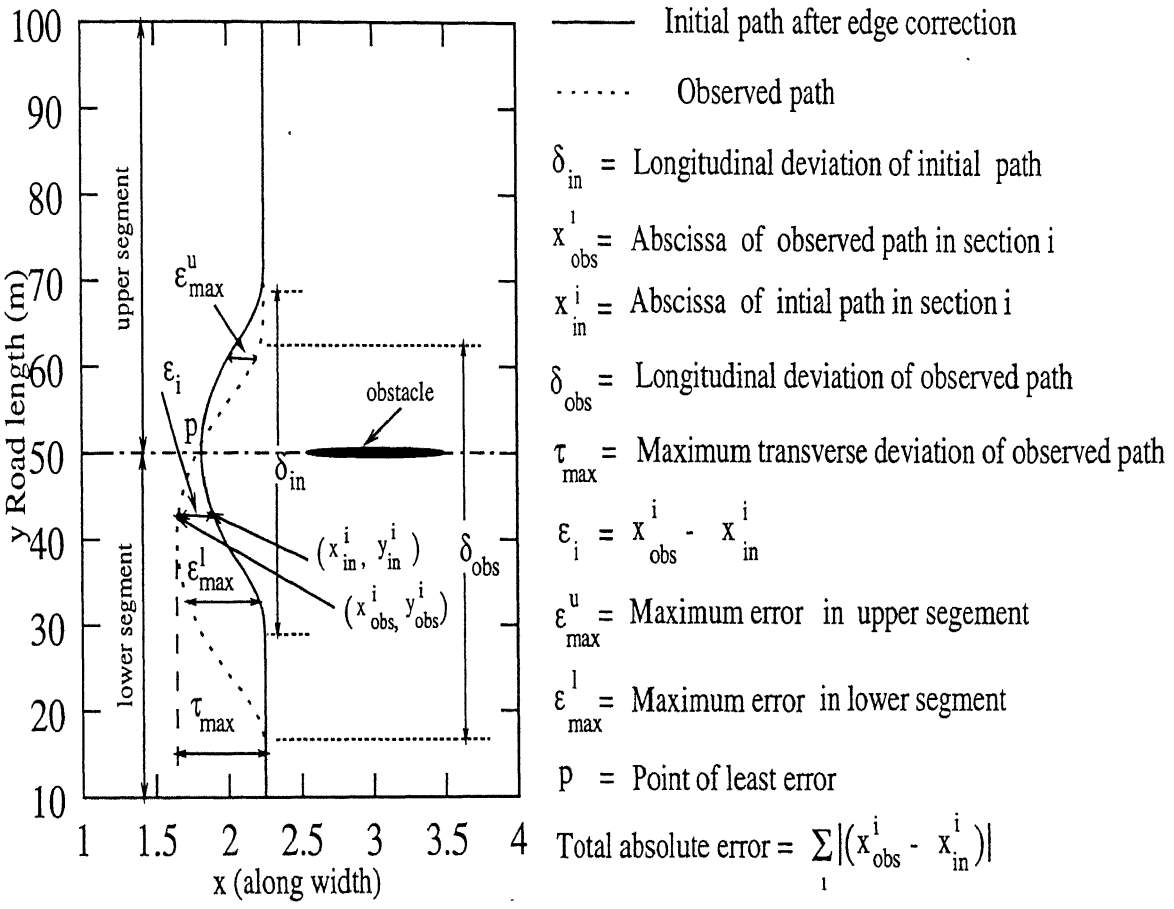

Figure 4.4: Illustration of the characteristics of the observed path and predicted path after Stage I calibration

1. Position of predicted path relative to observed path in a number of transverse sections in the obstacle influence zone.

2. Total absolute error between observed and predicted path obtained using:

   Total absolute error = $\sum_{\forall_i} |(X^i_{obs} - X^i_{in})|$, where "$i$" is a transverse section.

3. Maximum transverse deviation of observed path and predicted path and their location along the road stretch consider(see Figure 4.4).

4. Longitudinal deviation of observed path and predicted path (see Figure 4.4).

5. The point of least error (see Figure 4.4).

6. Maximum error in the upper part of the path and maximum error in lower part of the path.

These characteristics are measured in order help classify a particular scenario so that proper corrective actions can be taken. In the next section various scenarios (i.e. predicted path in comparison to observed path) are identified and the appropriate corrective actions in each of these cases are described.

4.3.2 Correction rules for the parameters of potential field function of obstacles

In this section the rules for the calibration of the parameter of the potential field function of static obstacle are presented. On studying the problem it was realized that a generalized calibration mechanism may not be feasible due to the complex nature of potential function and the way the parameters affect the path. Hence, it was decided to first classify a given condition (i.e., a given combination of the initially predicted path and the observed path) in to different "Situations." The classification is based on the characteristics define in the earlier section. However, for clarity of understanding the different situation are presented here schematically in Figure 4.5.

Classifications

In all the parts of the figure the vehicle is assumed to travel from bottom to top of the figure. Part (a) of the figure is referred to as Situation 1. In this situation the initial path lies totally to the left of the observed path. That is, both the transverse and longitudinal deviation of initial path are more than that of the observed path. Part (b) of the figure is referred to as Situation 2. In this situation the initial path lies completely to the right of observed path. Part (c) of the figure is referred to as Situation 3. In this situation the initial path intersect the observed path. Further, the initial path is farther from the obstacle in the upstream side of the obstacle and closer to the obstacle in the downstream side of the obstacle when compared to the observed path. Part (d) of the figure is Situation 4 and represents the exact opposite of Situation 3. Part (e) of the figure represents Situation 5. In this situation the initial path intersect the observed path twice. Further, the initial path is farther than the observed path in the vicinity of obstacle. Part (f) of the figure referred as

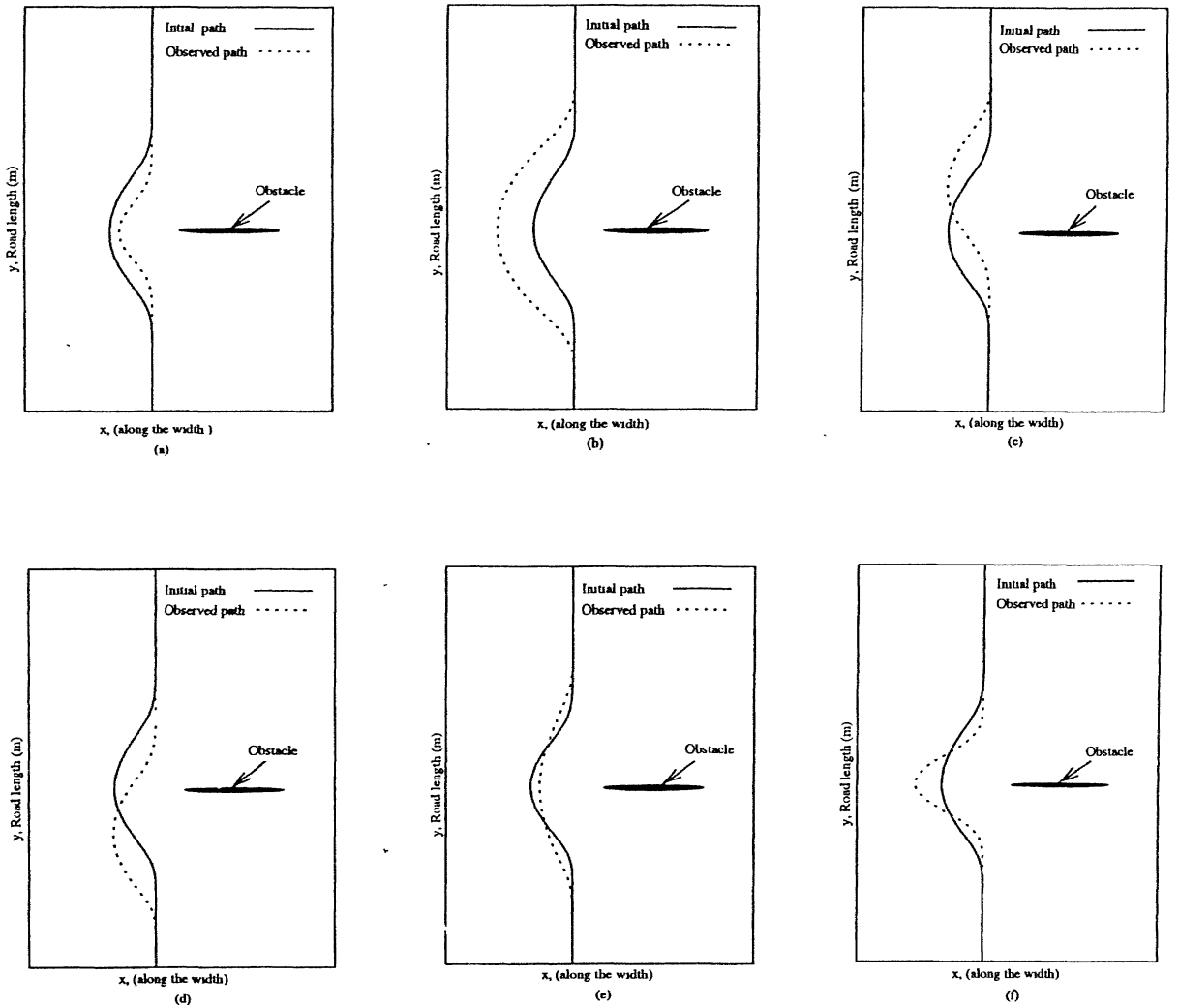

Figure 4.5: Classification of the comparison of the predicted path (after Stage I calibration) and the observed path

Situation 6 which is the opposite of Situation 5.

It may be pointed out here that from the standpoint of determining the rules of the calibration, there exists no difference between the situations shown in Figure 4.5 and their mirror images about a longitudinal axis. In the next section the rules for calibration for each of these situation are developed.

Rules of calibration

Here, the rules of calibration for the different situations are described. These rules are obtained from the understanding of the effect of different parameters on predicted path (see Chapter 3).

Situation 1: The rules are– (i) decrease a_4, (ii) decrease m_a, (iii) increase b_4, b_5 and ordinate of tp such that the slope function $f(y)$ takes a value greater than the initial value in every section, and (iv) if maximum error in upper segment, ϵ^u_{max}, is more than that in lower segment, ϵ^l_{max}, then decrease the abscissa value of tp and vice versa. Further, in this situation the rate of change of each parameter is kept same as them are equally effective in reducing in type of error seen in this situation. If however, $\epsilon^u_{max} > \epsilon^l_{max}$ then b_5 is change at a higher rate than b_4 and vice versa.

Situation 2: The rules are– (i) increase a_4, (ii) increase m_a, (iii) decrease b_4, b_5 and ordinate of tp such that the slope function $f(y)$ takes a value smaller than the initial value in every section, and (iv) if maximum error in upper segment, ϵ^u_{max}, is more than that in lower, ϵ^l_{max}, then decrease the abscissa value of tp and vice versa. Further, in this situation the rate of change of each parameter is kept same as them are equally effective in reducing in type of error seen in this situation. if however, $\epsilon^u_{max} > \epsilon^l_{max}$ then b_5 is change at a higher rate than b_4 and vice versa.

Situation 3: Unlike in Situation 1 and 2 simple rules for changing the parameter like a_4, m_a, b_4, b_5 and tp are not possible in this case. The reason for this is that the initial path's differences from the observed path have different characteristics in different segment. For example, the initial path has higher transverse deviation in the upstream side of obstacle but has lower transverse deviation in downstream side of obstacle when compare to observed path. Hence in this case the rules becomes slightly more complex. In following enumerated paragraphs the rules are described.

(i) In every iteration change m_a and a_4 in a manner such that the total absolute error (as explained in Section 5.14) reduces in that iteration.

(ii) Increase b_4 and decrease b_5 so that eventually the value of $f(y)$ is lower than initial value in the region where transverse deviation of initial path is lower than the observed path and vice versa.

(iii)Change the abscissa value of tp such that total absolute error reduces. The ordinate of tp is changed based on two factors (i) which of $|\epsilon^u_{max}|$ and $|\epsilon^l_{max}|$ is greater, and (ii) whether the greater of the has a negative or a positive sign. If the greater of has a positive sign then reduce the ordinate tp, if however, it has a negative sign then the ordinate of tp is increased.

Since parameter a_4 and m_a change the predicted path symmetrically with respect to transverse axis going through obstacle changes in these parameter play a small rule in reducing total absolute error. Hence in this situation parameter related to $f(y)$ are changed at a higher rate than a_4 and m_a.

Situation 4: Unlike in Situation 1 and 2 simple rules for changing parameter like a_4, m_a, b_4, b_5 and tp are not possible in this case. The reason for this is that the initial path's differences from the observed path have different characteristics in different segment. For example, the initial path has higher transverse deviation in the downstream side of obstacle but has lower transverse deviation in upstream side of obstacle when compare to observed path. Hence in this case the rules becomes slightly more complex. In following enumerated paragraphs the rules are described.

(i) In every iteration change m_a and a_4 in a manner such that total absolute error (as explained in section 5.14) reduces in that iteration.

(ii) Decrease b_4 and increase b_5 so that eventually the value of $f(y)$ is lower than the initial value in the region where transverse deviation of initial path is lower than the observed path and vice versa.

(iii) Change the abscissa value of tp such that total absolute error reduces. The ordinate of tp is change based on two factors (i) which of $|\epsilon^u_{max}|$ and $|\epsilon^l_{max}|$ is greater, and (ii) whether the greater of the has a negative or a positive sign. If the greater has a positive sign then reduce the ordinate of tp, if however, it has a negative sign then ordinate of tp is increased.

Since parameter a_4 and m_a change the predicted path symmetrically with respect to transverse axis going through obstacle changes in these parameter play a small rule in reducing total absolute

error. Hence in this situation parameter related to $f(y)$ are changed at a higher rate than a_4 and m_a.

Situation 5: The rules are– (i) decrease a_4 (since maximum transverse deviation of initial path is more than of observed path), (ii) increase m_a (because longitudinal deviation of initial path, δ_{in} is less than longitudinal deviation of observed path, δ_{obs}), (iii) move the abscissa of tp in the direction of ordinate value of the point of maximum transverse deviation of the observed path, (iv) change b_4, b_5 and ordinate value of tp such that total error reduces.

Since parameter m_a is more effective in reducing the type of error seen in this situation. Hence in this situation m_a is changed at higher rate than the other parameters.

Situation 6: The rules are– (i) increase a_4 (since maximum transverse deviation of initial path is less than of observed path), (ii) decrease m_a (because longitudinal deviation of initial, δ_{in} is more than longitudinal deviation of observed path, δ_{obs}), (iii) move the abscissa of tp in the direction of ordinate value of the point of maximum transverse deviation of observed path, (iv) change b_4, b_5 and ordinate value of tp such that total error reduces.

Since parameter m_a is more effective in reducing the type of error seen in this situation. Hence is this situation m_a is changed at higher rate than the other parameters.

Chapter 5

RESULTS

In this chapter results are presented to show that the proposed calibration mechanism can successfully calibrated the parameters of the potential functions. Thirteen different cases are studied here. Schematics of these cases are shown in Figure 5.1 as case (a) through case (m). The abscissa of each schematics is the distance along the width of the road from the left edge and the ordinate is the distance along the length of the road. The solid line in the figure is the predicted path from the potential field theory based model of driver behavior before calibration and the broken line is the observed path which can be obtained from real word observations. The solid object in the figure represents the obstacle. The motivation for choosing these cases for studying is that they represent all possible realistic combination of the initial predicted path and observed path.

In the following, the results are shown for each of these thirteen cases. For each of these cases, expect for case (m) road width = 6 m, with the left edge assumed at 0 m, obstacle is a circle of diameter 1 m and the center is placed at (50, 3). For case (m) only the placement of the obstacle is different; the center of the obstacle in this case is at (50, 2.3). The results for each case are presented using the following formate. First, a set of two figures marked (a) and (b) are presented. In the figures the solid line represents the path obtained using the potential field theoretical model with an initial (uncalibrated) set of parameter values. The dotted line is a hypothetical path representing (in theory) the observed path (which in practice will be obtained from real world data). The dashed line represents the path obtained using the potential field theoretical model with the calibrated parameter values. The figure marked (a) only presents the initial and observed paths. The figure marked (b) present the initial, observed and calibrated paths.

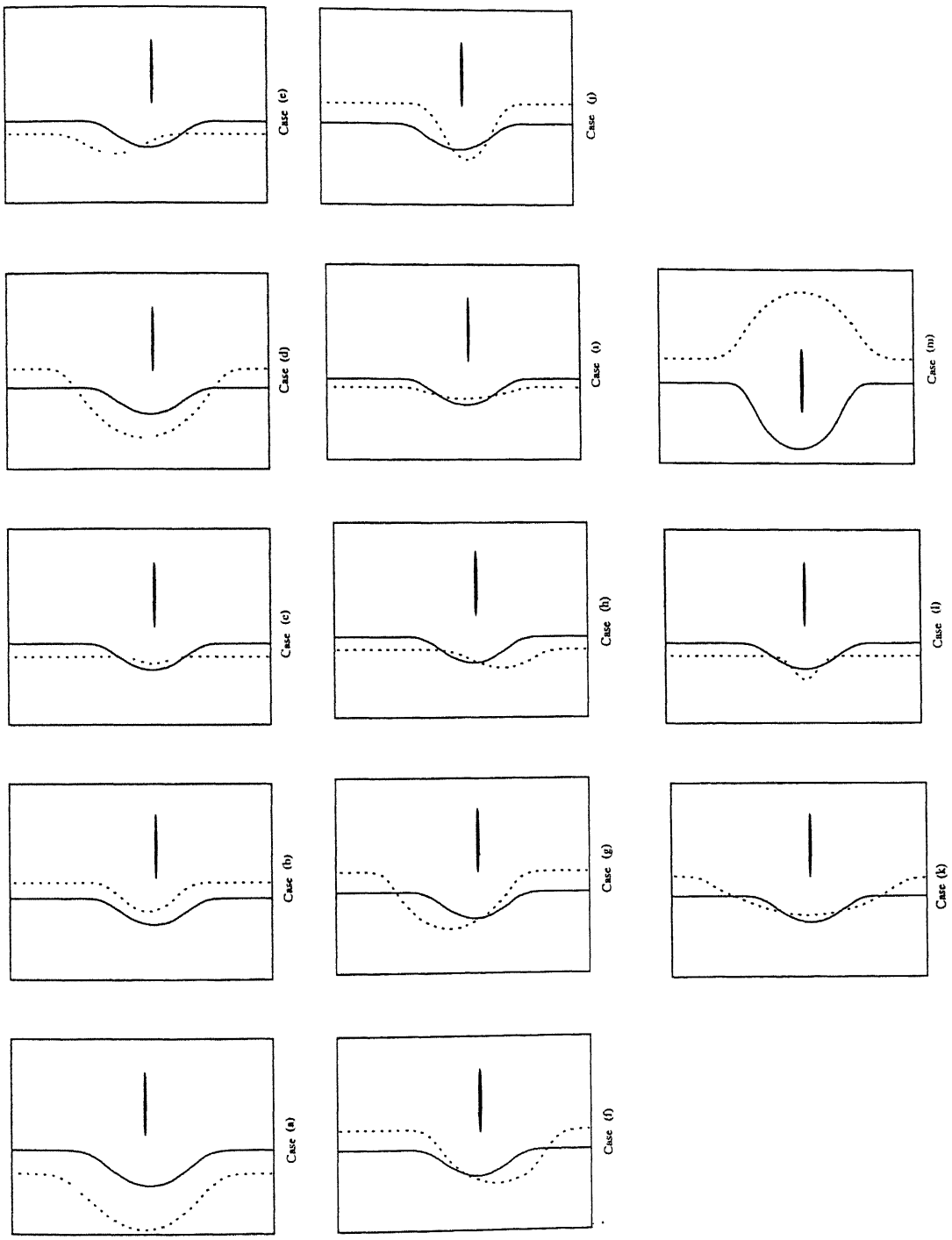

Figure 5.1: Cases studied in this chapter

Second, for each case a table is provided which gives the initial parameter values and the calibrat values.

1. **Case (a)**

   Figure 5.2 presents the result obtained using the proposed calibration mechanism. It c be seen from figure that even though there exists reasonable difference between the initial a observed path, after calibration the calibrated path is very close to the observed path. Table 5 presents the initial and calibrated values of the parameters of the potential field theory mod

Table 5.1: Initial and calibrated parameter values for Case (a)

Parameters of the potential functions	Parameter values	
	Initially assumed	After calibration
a_1	1.0	0.9110
b_1	0.32641	0.327332
a_2	4.0	4.089002
b_2	0.04663	0.045745
a_4	2.0	3.292
m_a	8.0	8.940
b_4	2.0	1.952241
t_1	0.0	0.0
α	0.0	-0.000005
β	0.0	0.001139
γ	0.0	-0.071770
δ	2.0	1.952241
b_5	2.0	1.640931
t_2	100.0	100.0
$tp\ (x, y)$	(50.0, 2.0)	(42.10, 0.61)

2. **Case (b)**

   Figure 5.3 presents the result obtained using the proposed calibration mechanism. It can seen from the figure that even though there exists reasonable difference between the initial a observed path, after calibration the calibrated path is very close to the observed path. Table presents the initial and calibrated values of the parameters of the potential field theory mod

3. **Case (c)**

   Figure 5.4 presents the result obtained using the proposed calibration mechanism. It can seen from the figure that even though there exists reasonable difference between the initial

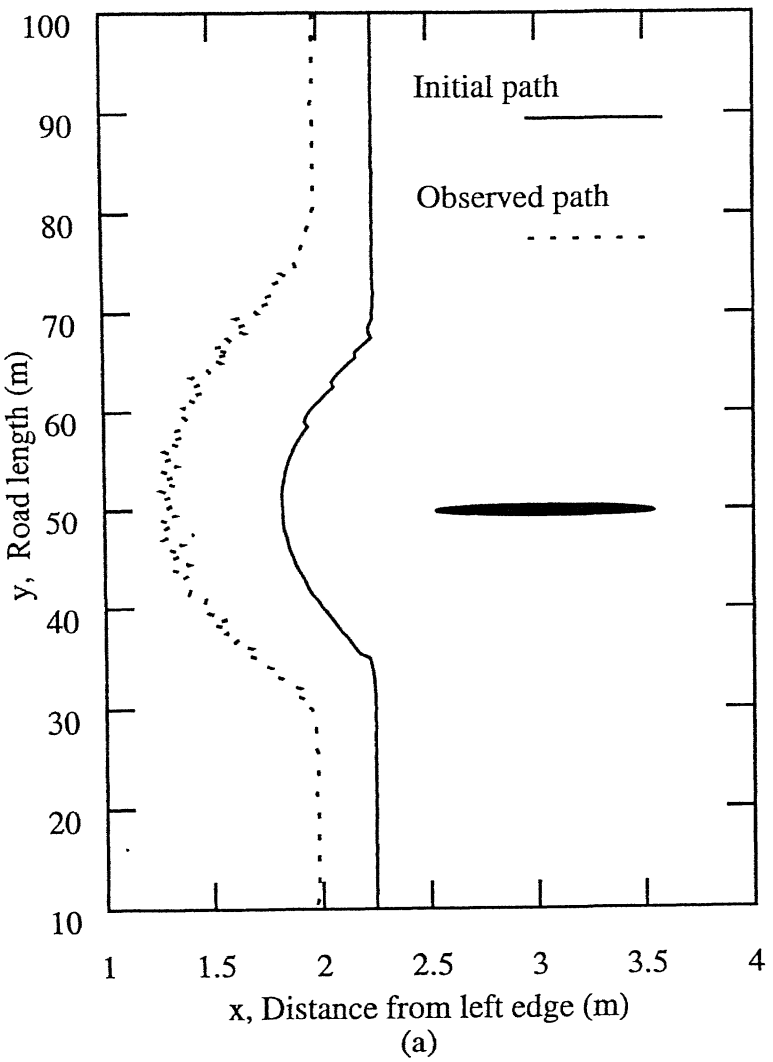

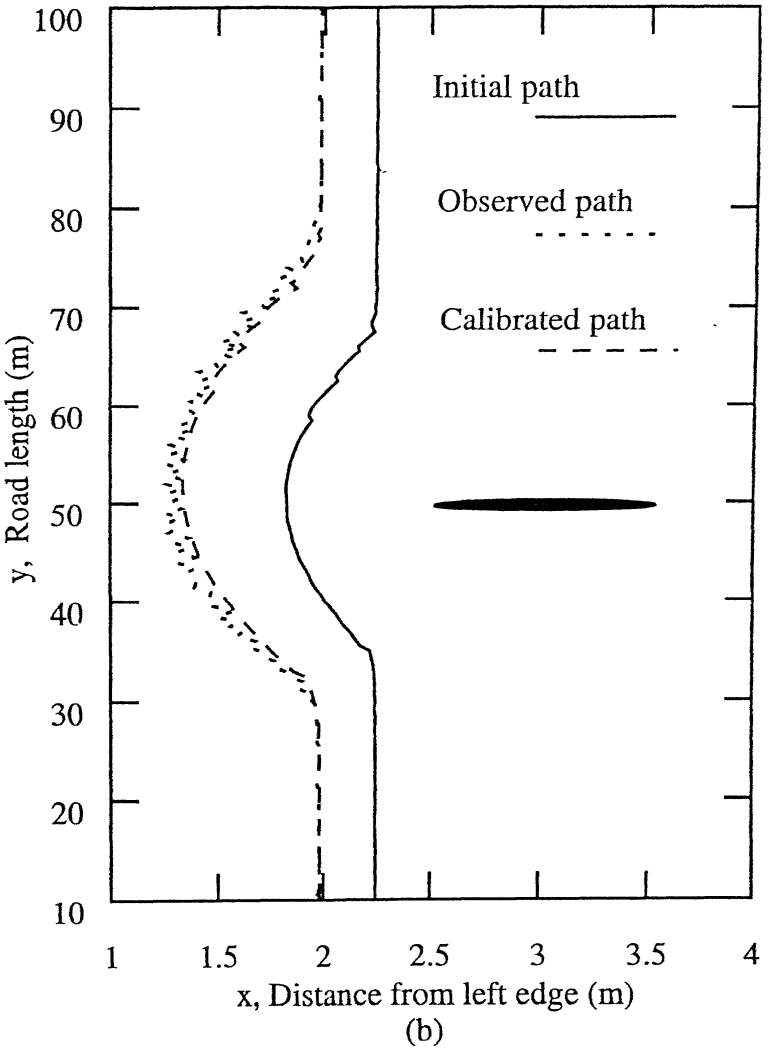

Figure 5.2: Result showing (a) the initial and observed paths and (b) the initial, observed and calibrated paths for Case (a)

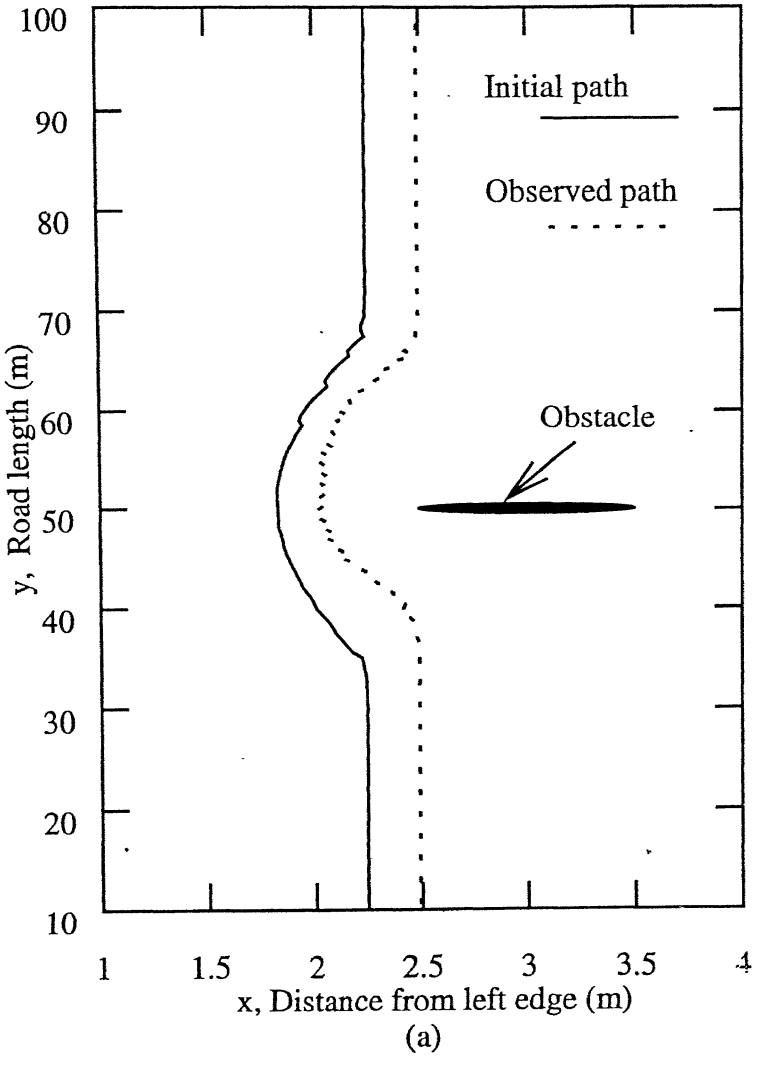

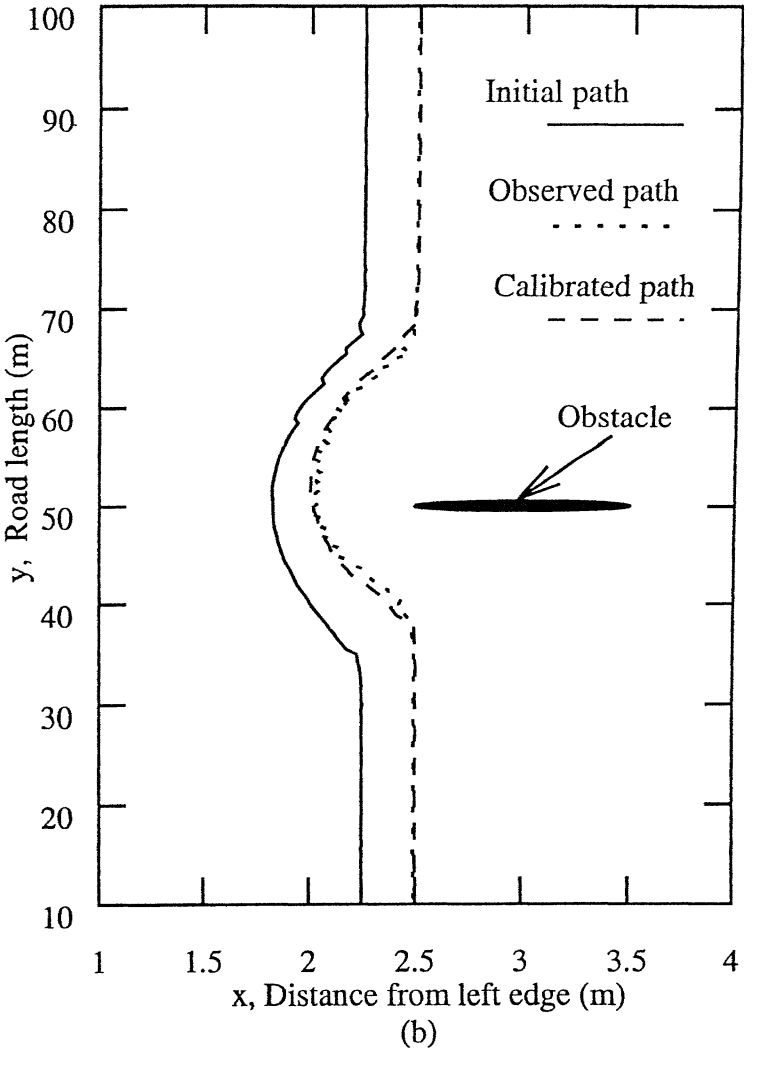

Figure 5.3: Result showing (a) the initial and observed paths and (b) the initial, observed and calibrated paths for Case (b)

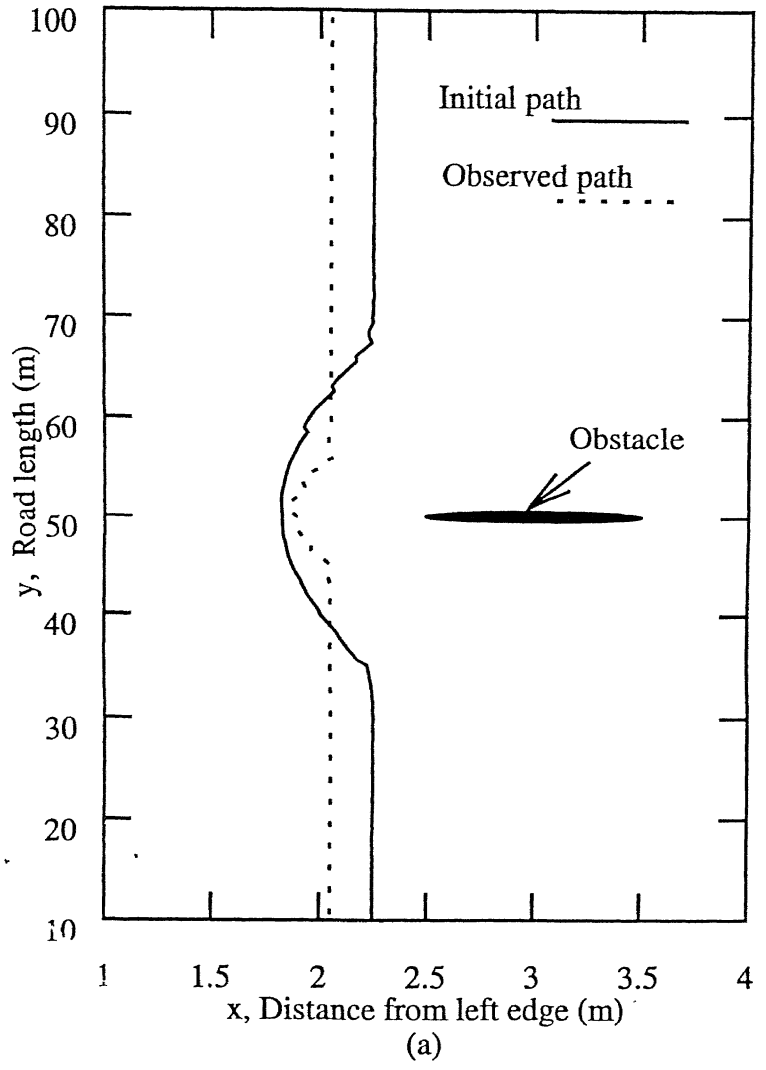

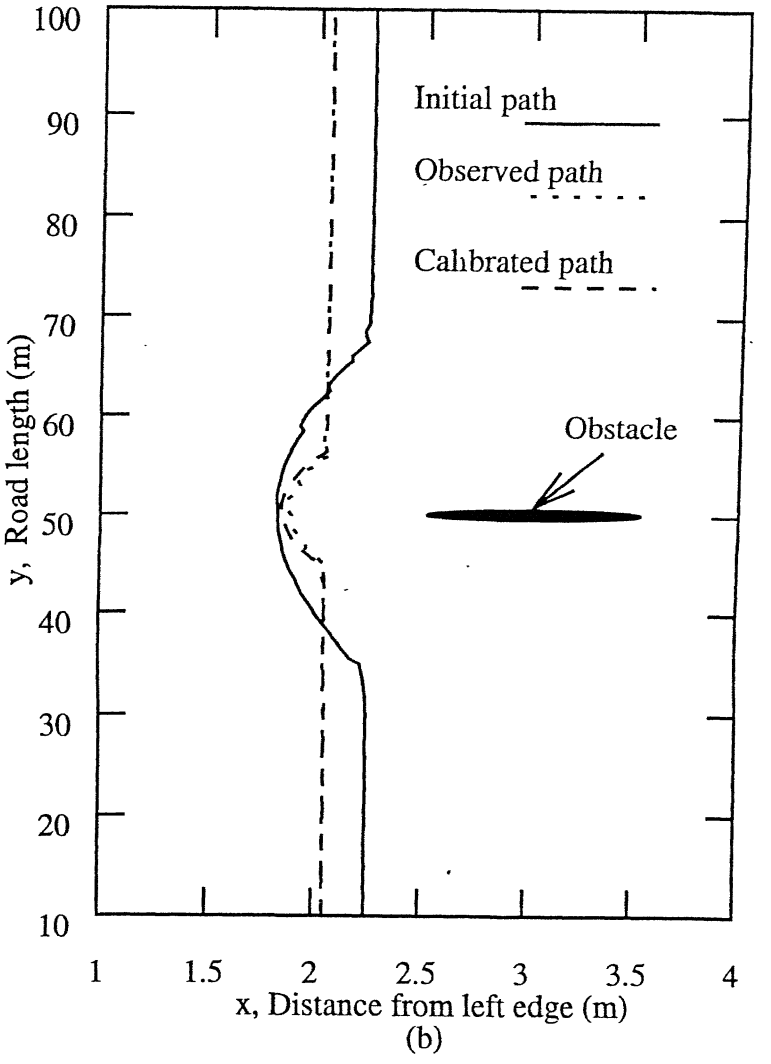

Figure 5.4: Result showing (a) the initial and observed paths and (b) the initial, observed and calibrated paths for Case (c)

Table 5.2: Initial and calibrated parameter values for Case (b)

Parameters of the potential functions	Parameter values	
	Initially assumed	After calibration
a_1	1.0	1.0890
b_1	0.32641	0.32553
a_2	4.0	3.91100
b_2	0.04663	0.047525
a_4	2.0	1.65
m_a	8.0	7.6500
b_4	2.0	2.570301
t_1	0.0	0.0
α	0.0	-0.000004
β	0.0	0.000337
γ	0.0	0.002987
δ	2.0	2.570301
b_5	2.0	2.274796
t_2	100	100.0
$tp\ (x, y)$	(50.0, 2.0)	(60.45, 3.10)

and observed path, after calibration the calibrated path is very close to the observed path. Table 5.3 presents the initial and calibrated values of the parameters of the potential field theory model.

Table 5.3: initial and calibrated parameter values for Case (c)

Parameters of the potential functions	Parameter values	
	Initially assumed	After calibration
a_1	1.0	0.9330
b_1	0.32641	0.32712
a_2	4.0	4.067002
b_2	0.04663	0.045962
a_4	2.0	1.3567
m_a	8.0	6.3900
b_4	2.0	3.729918
t_1	0.0	0.0
α	0.0	0.0
β	0.0	0.000648
γ	0.0	-0.062219
δ	2.0	3.7299918
b_5	2.0	3.755372
t_2	100.0	100.0
$tp\ (x, y)$	(50.0, 2.0)	(49.34, 2.21)

4. **Case (d)**

Figure 5.5 presents the result obtained using the proposed calibration mechanism. It can be seen from the figure that even though there exists reasonable difference between the initial

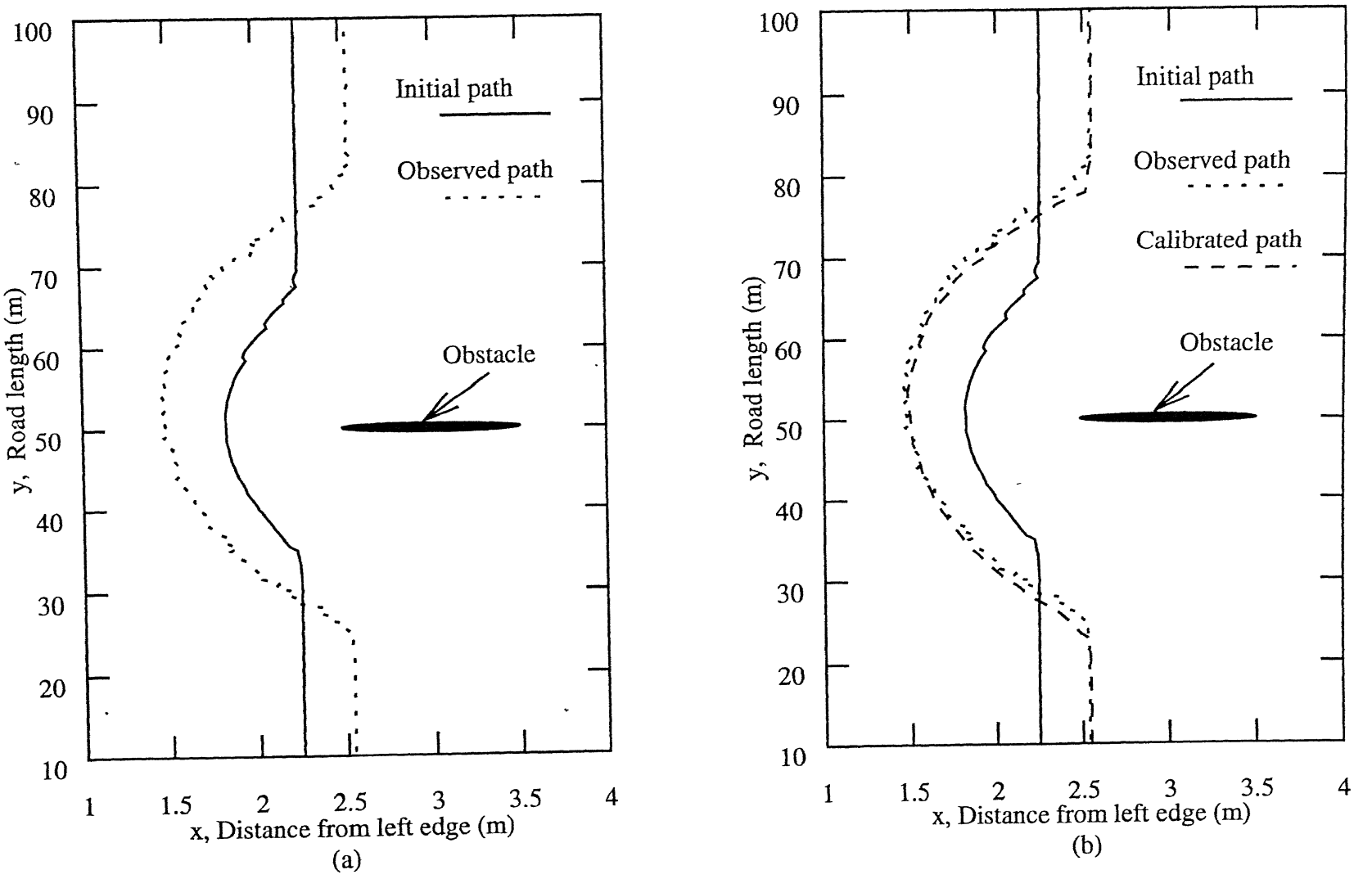

Figure 5.5: Result showing (a) the initial and observed paths and (b) the initial, observed and calibrated paths for Case (d)

and observed path, after calibration the calibrated path is very close to the observed path. Table 5.4 presents the initial and calibrated values of the parameters of the potential field theory model.

Table 5.4: Initial and calibrated parameter values for Case (d)

Parameters of the potential functions	Parameter values	
	Initially assumed	After calibration
a_1	1.0	1.120
b_1	0.32641	0.325243
a_2	4.0	3.8800
b_2	0.04663	0.047835
a_4	2.0	3.6440
m_a	8.0	9.39992
b_4	2.0	1.610029
t_1	0.0	0.0
α	0.0	-0.000004
β	0.0	0.000872
γ	0.0	-0.050558
δ	2.0	1.610029
b_5	2.0	1.228277
t_2	100.0	100.0
$tp = (x, y)$	(50.0, 2.0)	(40.35, 0.723)

5. **Case (e)**

   Figure 5.6 presents the result obtained using the proposed calibration mechanism. It can be seen from the figure that even though there exists reasonable difference between the initial and observed path, after calibration the calibrated path is very close to the observed path. Table 5.5 presents the initial and calibrated values of the parameters of the potential field theory model.

6. **Case (f)**

   Figure 5.7 presents the result obtained using the proposed calibration mechanism. It can be seen from the figure that even through there exists reasonable difference between the initial and observed path, after calibration the calibrated path is very close to the observed path. Table 5.6 presents the initial and calibrated values of the parameters of the potential field theory model.

7. **Case (g)**

   Figure 5.8 presents the result obtained using the proposed calibration mechanism. It can be seen from the figure that even though there exists reasonable difference between the initial and

Table 5.5: Initial and calibrated parameter values for Case (e)

Parameters of the potential functions	Parameter values	
	Initially assumed	After calibration
a_1	1.0	0.93300
b_1	0.32641	0.32712
a_2	4.0	4.067002
b_2	0.04663	0.045962
a_4	2.0	1.867
m_a	8.0	8.950
b_4	2.0	3.20001
t_1	0.0	0.0
α	0.0	0.000021
β	0.0	-0.002864
γ	0.0	0.071480
δ	2.0	3.200001
b_5	2.0	3.11968
tp	100.0	100.0
$tp\ (x, y)$	(50.0, 2.0)	(15.0, 3.7)

Table 5.6: Initial and calibrated parameter values for Case (f)

Parameters of the potential functions	Parameter values	
	Initially assumed	After calibration
a_1	1.0	1.120
b_1	0.32641	0.325243
a_2	4.0	3.880
b_2	0.04663	0.047835
a_4	2.0	2.385
m_a	8.0	8.799910
b_4	2.0	0.581535
t_1	0.0	0.0
α	0.0	0.000005
γ	0.0	0.000182
β	0.0	-0.005492
δ	2.0	0.581535
b_5	2.0	7.107835
t_2	100.0	100.0
$tp = (x, y)$	(50.0, 2.0)	(10.40, 0.55)

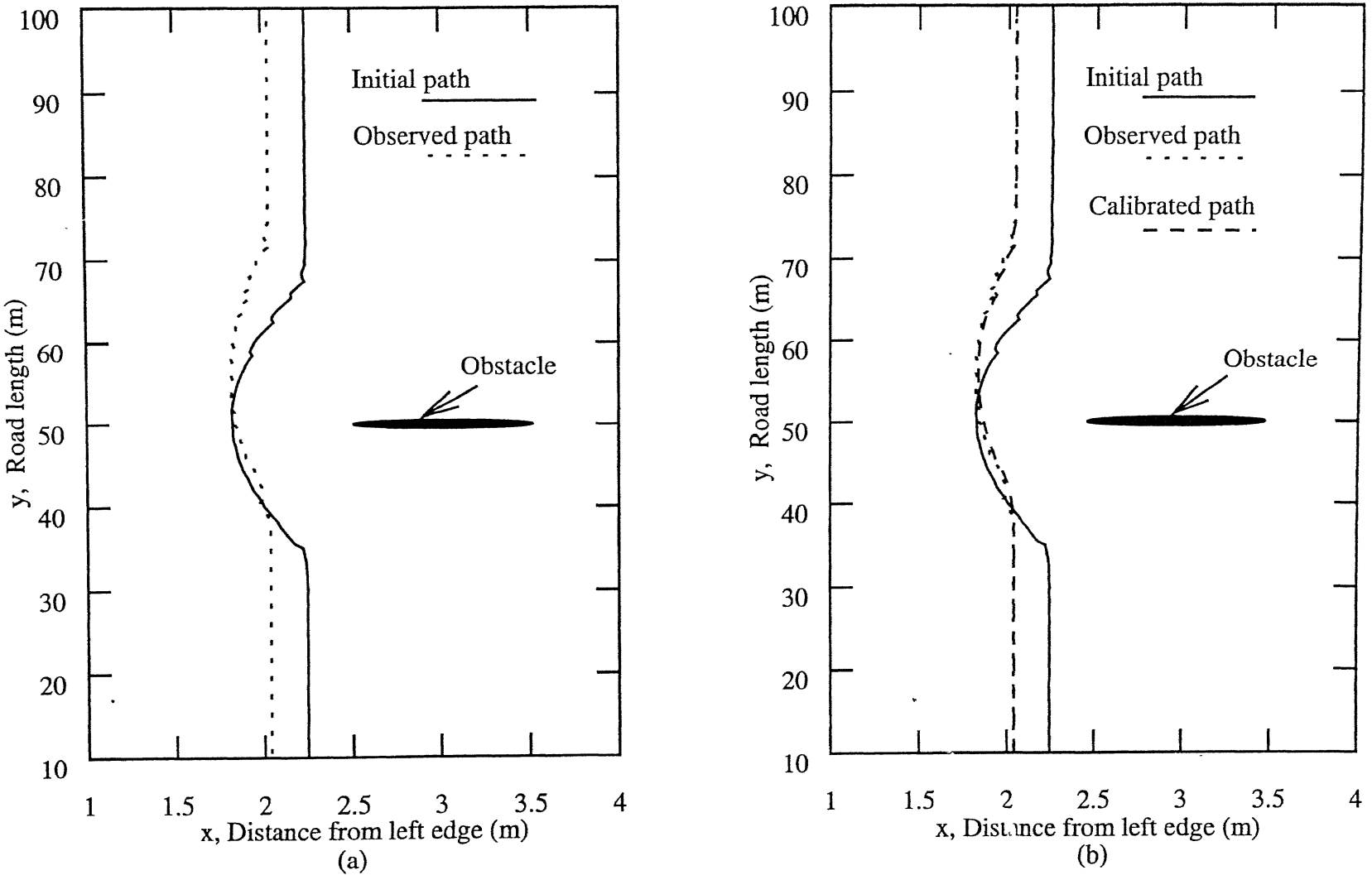

Figure 5.6: Result showing (a) the initial and observed paths and (b) the initial, observed and calibrated paths for Case (e)

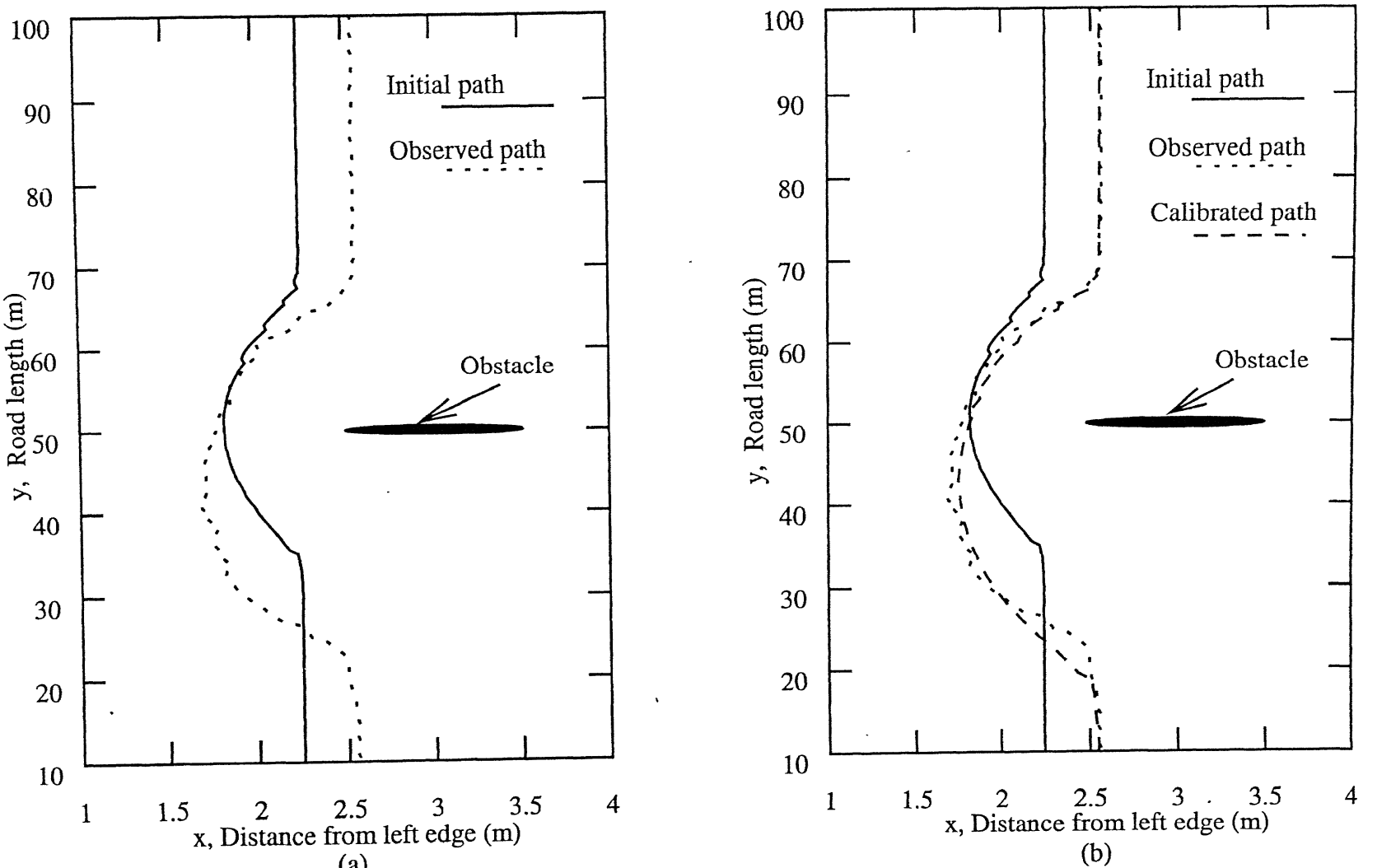

Figure 5.7: Result showing (a) the initial and observed paths and (b) the initial, observed and calibrated paths for Case (f)

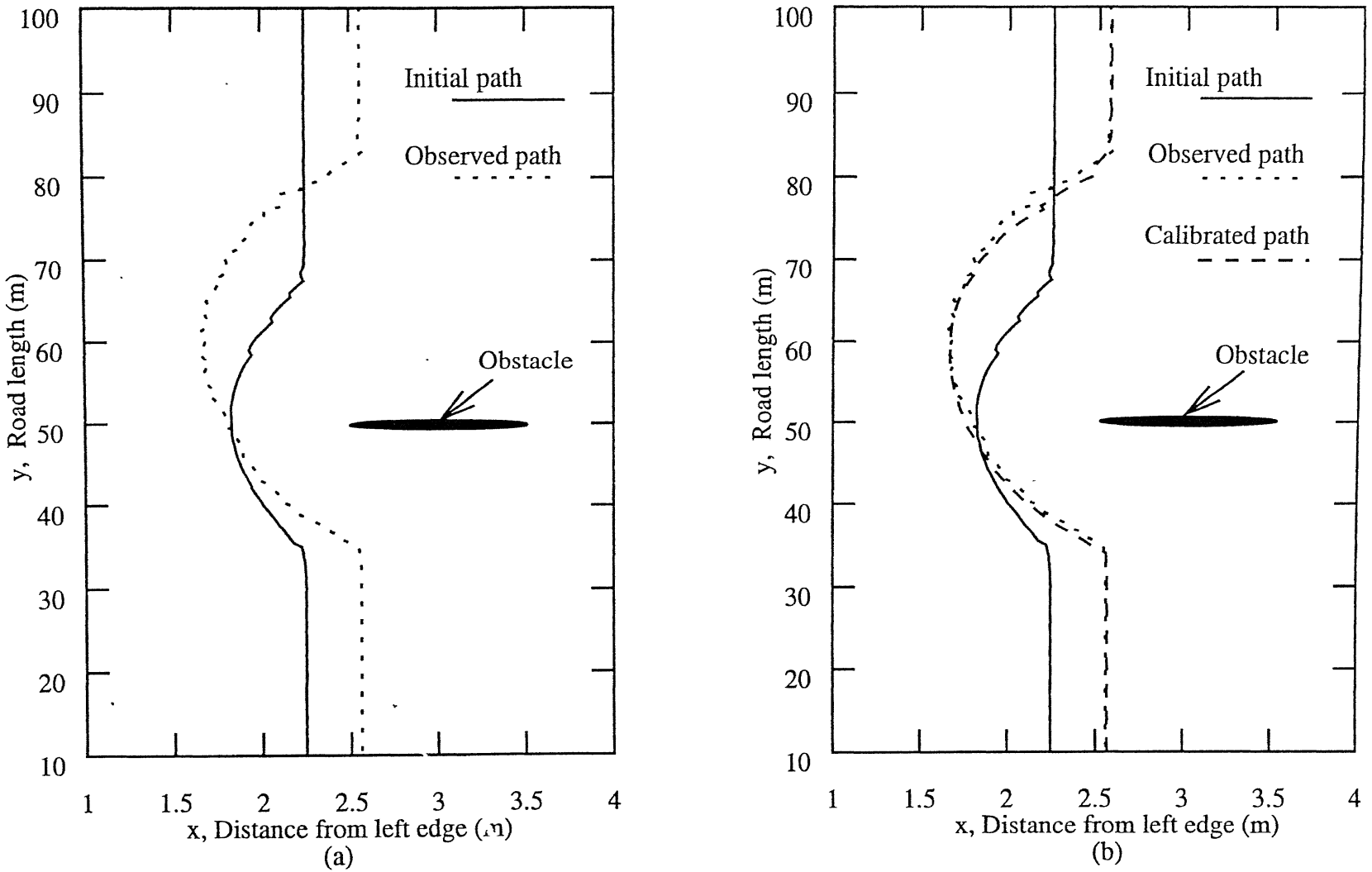

Figure 5.8: Result showing (a) the initial and observed paths and (b) the initial, observed and calibrated paths for Case (g)

observed path, after calibration the calibrated path is very close to the observed path. Table 5.7 presents the initial and calibrated values of the parameters of the potential field theory model.

Table 5.7: Initial and calibrated parameter values for Case (g)

Parameters of the potential functions	Parameter values	
	Initially assumed	After calibration
a_1	1.0	1.120
b_1	0.32641	0.325243
a_2	4.0	3.8800
b_2	0.04663	0.047835
a_4	2.0	1.88500
m_a	8.0	8.51
b_4	2.0	9.162707
t_1	0.0	0.0
α	0.0	-0.000012
β	0.0	0.003222
γ	0.0	-0.289156
δ	2.0	9.162707
b_5	2.0	0.703910
t_2	100.0	100.0
$tp = (x, y)$	(50.0, 2.0)	(85.10, 0.51)

8. **Case (h)**

   Figure 5.9 presents the result obtained using the proposed calibration mechanism. It can be seen from the figure that even though there exists reasonable difference between the

   initial and observed path, after calibration the calibrated path is very close to the observed path. Table 5.8 presents the initial and calibrated values of the parameters of the potential field theory model.

9. **Case (i)**

   Figure 5.10 presents the result obtained using the proposed calibration mechanism. It can be seen from the figure that even though there exists reasonable difference between the initial and observed path, after calibration the calibrated path

   is very close to the observed path. Table 5.9 presents the initial and calibrated values of the parameters of the potential field theory model.

10. **Case (j)**

    Figure 5.11 presents the result obtained using the proposed calibration mechanism. It can be seen from the figure that even though there exists reasonable difference between the initial

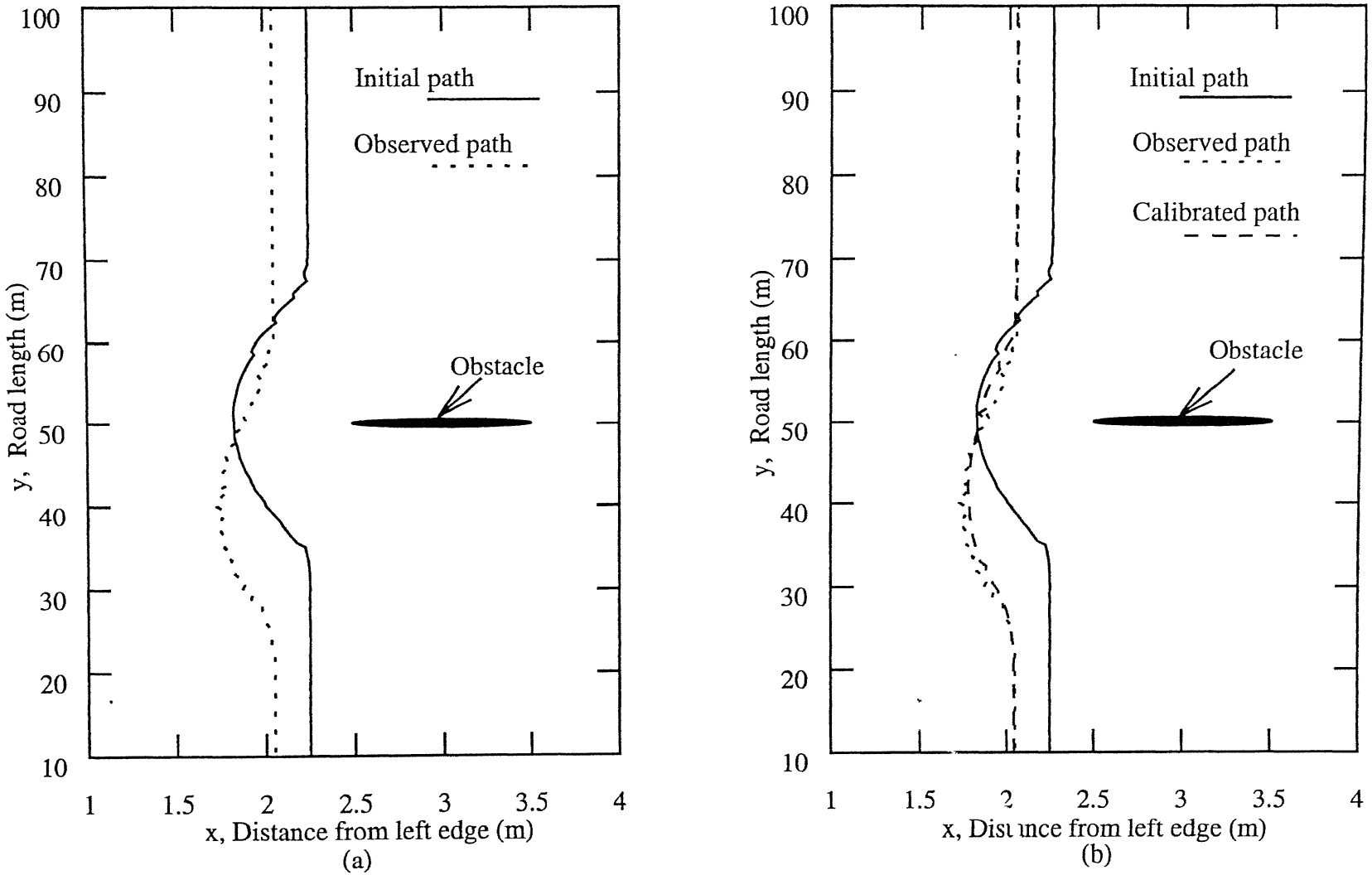

Figure 5.9: Result showing (a) the initial and observed paths and (b) the initial, observed and calibrated paths for Case (h)

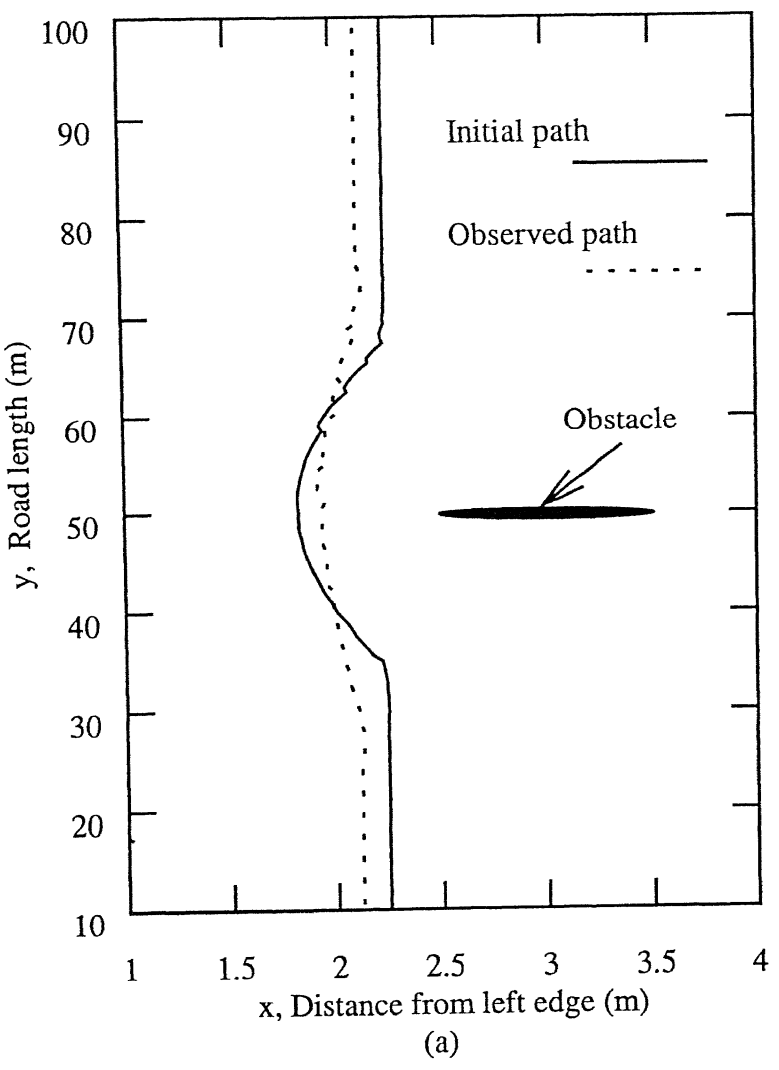

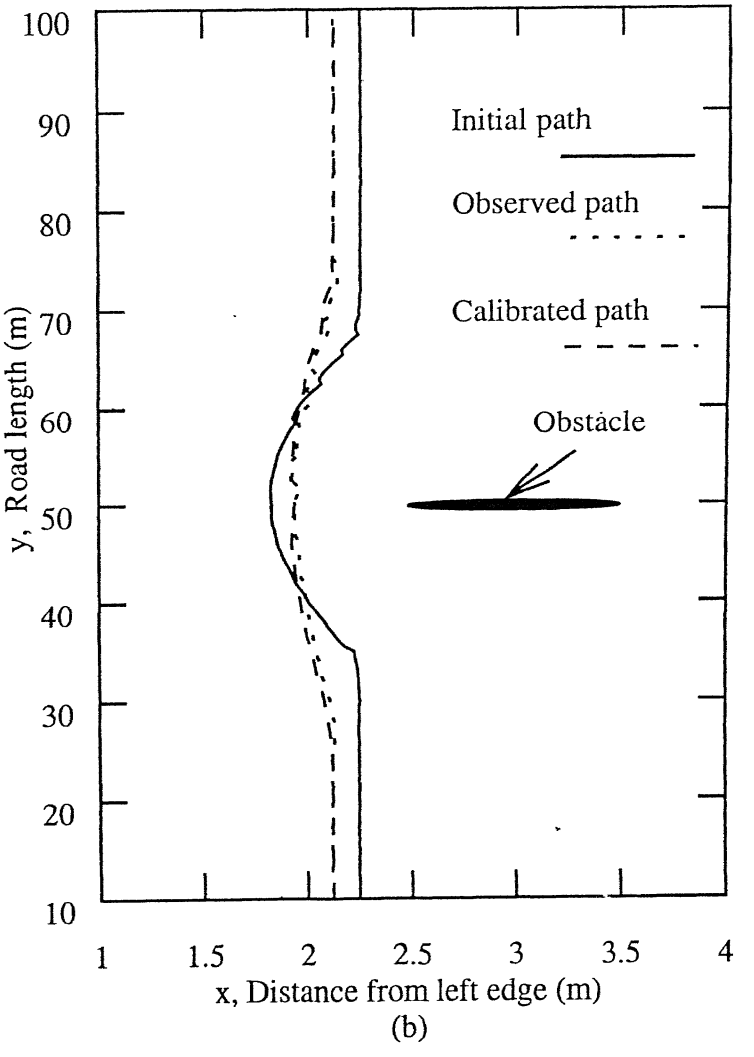

Figure 5.10: Result showing (a) the initial and observed paths and (b) the initial, observed and calibrated paths for Case (i)

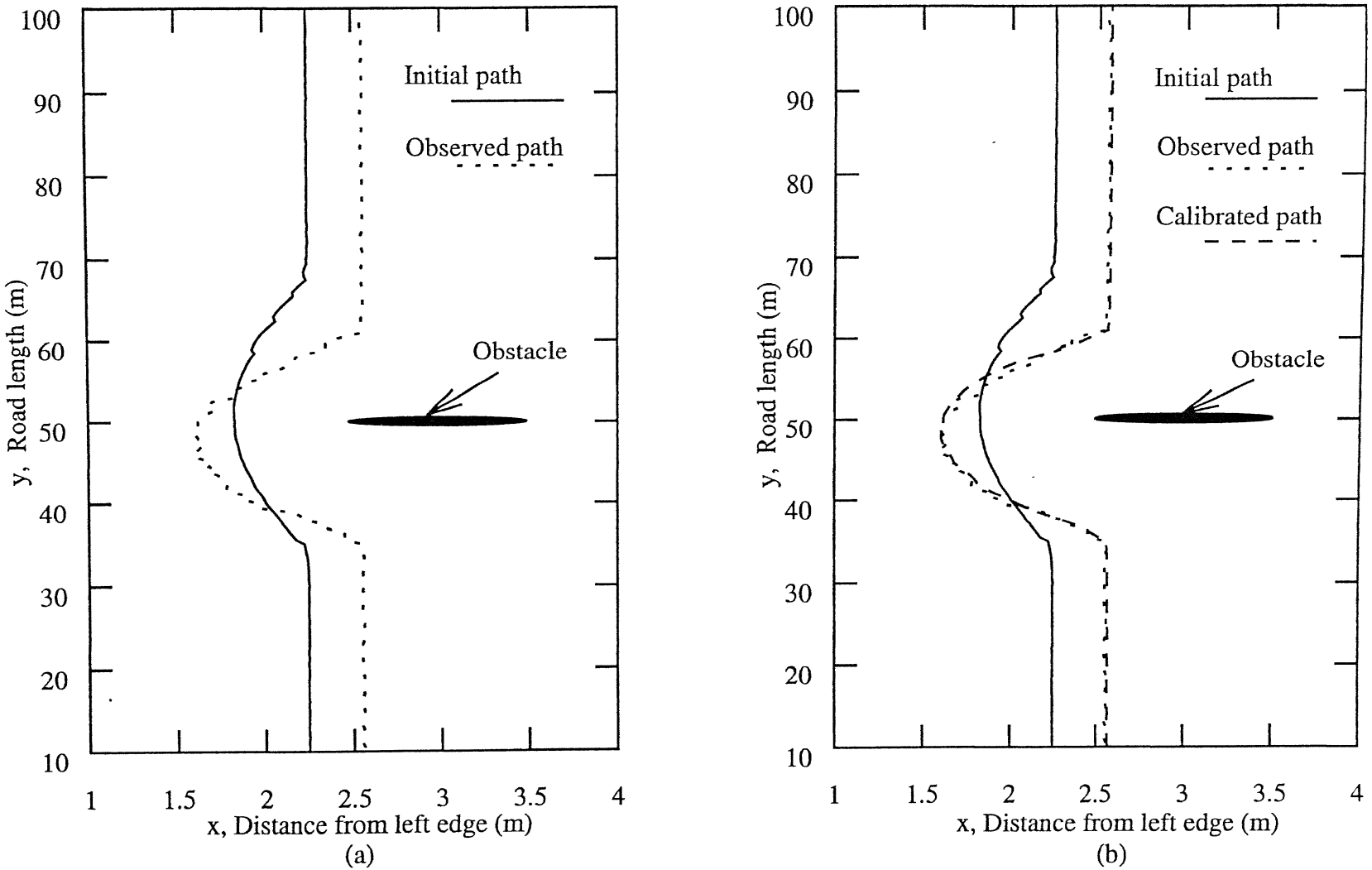

Figure 5.11: Result showing (a) the initial and observed paths and (b) the initial, observed and calibrated paths for Case (j)

Table 5.8: Initial and calibrated parameter values for Case (h)

Parameters of the potential functions	Parameter values	
	Initially assumed	After calibration
a_1	1.0	0.9330
b_1	0.32641	0.32712
a_2	4.0	4.067002
b_2	0.04663	0.045965
a_4	2.0	1.899
m_a	8.0	8.9500
b_4	2.0	2.900171
t_1	0.0	0.0
α	0.0	-0.000027
β	0.0	0.004457
γ	0.0	-0.180238
δ	2.0	2.900171
b_5	2.0	2.899993
t_2	100.0	2.818590
$tp\ (x, y)$	(50.0, 2.0)	(85.15, 3.40)

Table 5.9: Initial and calibrated parameter values for Case (i)

Parameters of the potential functions	Parameter values	
	Initially assumed	After calibration
a_1	1.0	0.95500
b_1	0.32641	0.326892
a_2	4.0	4.045002
b_2	0.04663	0.046185
a_4	2.0	1.867
m_a	8.0	12.54
b_4	2.0	1.30
t_1	0.0	0.0
α	0.0	0.0
β	0.0	-0.000517
γ	0.0	0.049223
δ	2.0	1.300001
b_5	2.0	1.30279
t_2	100.0	100.0
$tp\ (x, y)$	(50.0, 2.0)	(49.36, 2.5)

and observed path, after calibration the calibrated path is very close to the observed path. Table 5.10 presents the initial and calibrated values of the parameters of the potential field theory model.

Table 5.10: Initial and calibrated parameter values for Case (j)

Parameters of the potential functions	Parameter values	
	Initially assumed	After calibration
a_1	1.0	1.12
b_1	0.32641	0.325243
a_2	4.0	3.8800
b_2	0.04663	0.047835
a_4	2.0	4.94300
m_a	8.0	5.09910
b_4	2.0	2.79625
t_1	0.0	0.0
α	0.0	-0.000001
β	0.0	0.001339
γ	0.0	-0.101512
δ	2.0	2.79625
b_5	2.0	4.74830
t_2	100.0	100.0
$tp\ (x,y)$	(50.0, 2.0)	(40.21, 0.796)

11. **Case (k)**

Figure 5.12 presents the result obtained using the proposed calibration mechanism. It can be seen from the figure that even though there exists reasonable difference between the initial and observed path, after calibration the calibrated path is very close to the observed path. Table 5.11 presents the initial and calibrated values of the parameters of the potential field theory model.

12. **Case (l)**

Figure 5.13 presents the result obtained using the proposed calibration mechanism. It can be seen from the figure that even though there exists reasonable difference between the initial and observed path, after calibration the calibrated path is very close to the observed path. Table 5.12 presents the initial and calibrated values of the parameters of the potential field theory model.

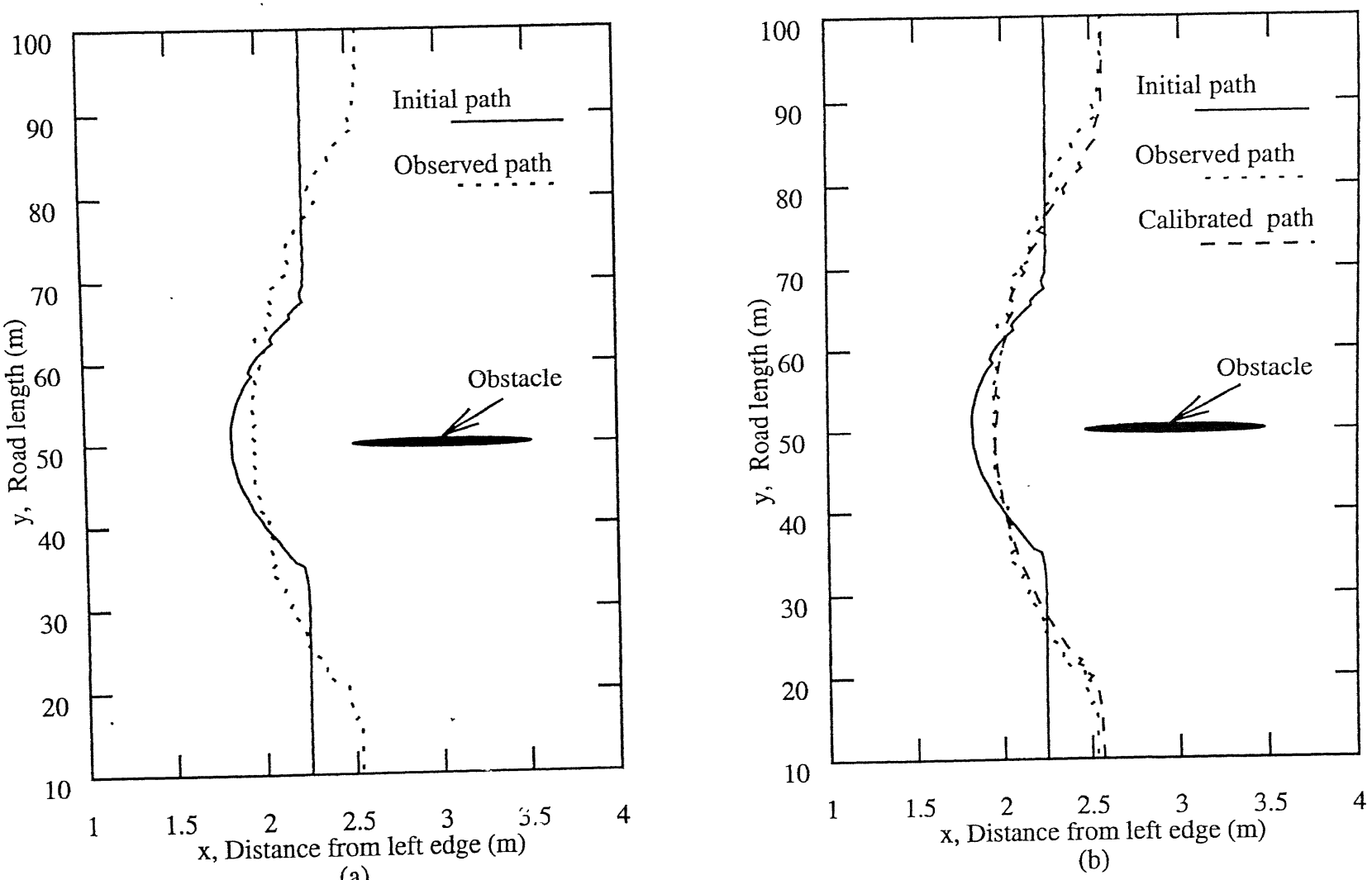

Figure 5.12: Result showing (a) the initial and observed paths and (b) the initial, observed and calibrated paths for Case (k)

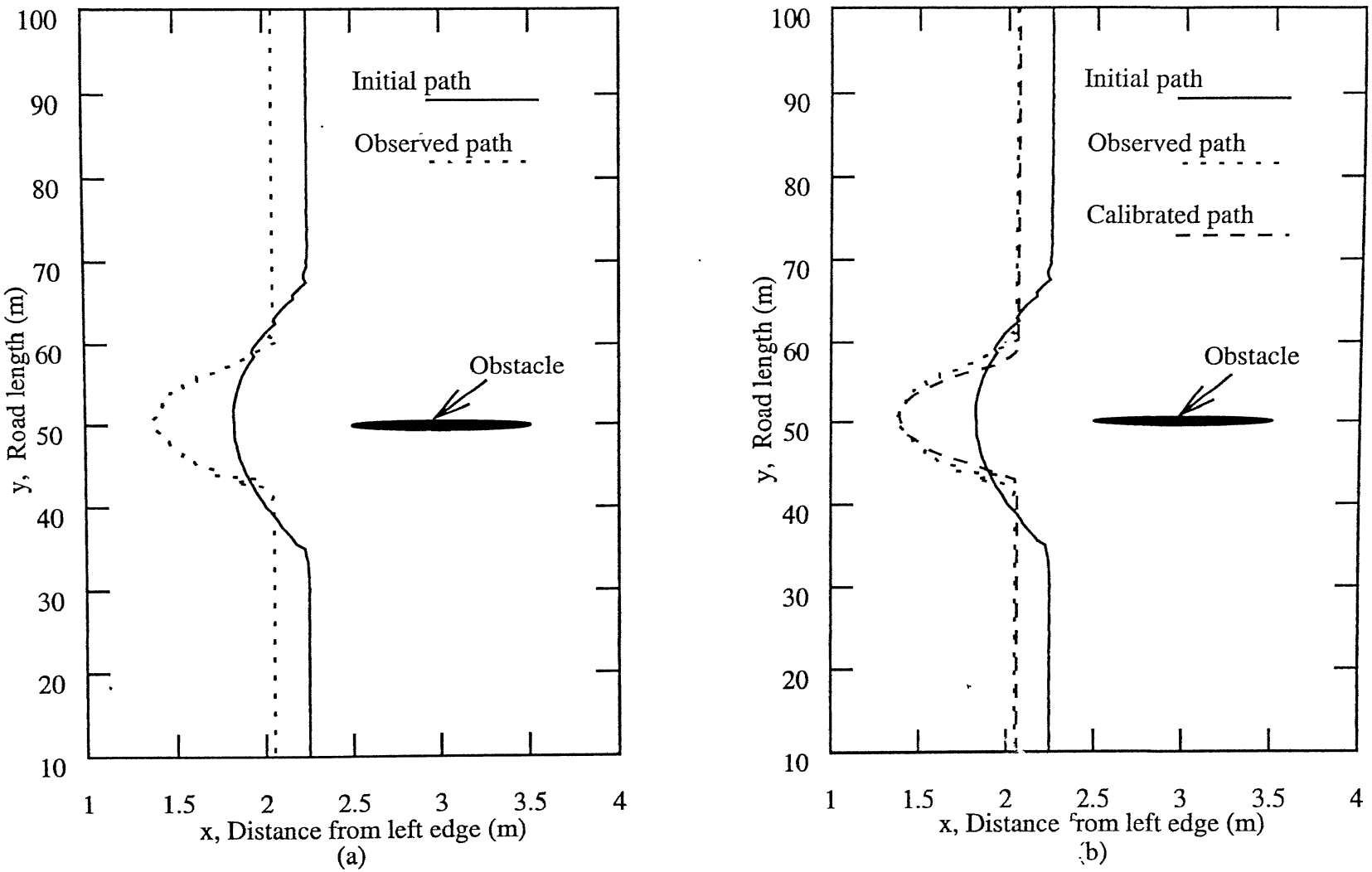

Figure 5.13: Result showing (a) the initial and observed paths and (b) the initial, observed and calibrated paths for Case (l)

Table 5.11: Initial and calibrated parameter values for Case (k)

Parameters of the potential functions	Parameter values	
	Initially assumed	After calibration
a_1	1.0	1.120
b_1	0.32641	0.325243
a_2	4.0	3.8800
b_2	0.04663	0.427835
a_4	2.0	1.885
m_a	8.0	13.98600
b_4	2.0	1.490010
t_1	0.0	0.0
α	0.0	0.000002
β	0.0	-0.000610
γ	0.0	0.039099
δ	2.0	1.490010
b_5	2.0	1.361133
t_2	100.0	100.0
$tp = (x, y)$	(50.0, 2.0)	(40.25, 2.21)

Table 5.12: Initial and calibrated parameter values for Case (l)

Parameters of the potential functions	Parameter values	
	Initially assumed	After calibration
a_1	1.0	0.9330
b_1	0.32641	0.32712
a_2	4.0	4.067002
b_2	0.04663	0.045962
a_4	2.0	4.0200
m_a	8.0	4.3900
b_4	2.0	1.96097
t_1	0.0	0.0
α	0.0	0.000001
β	0.0	0.000372
γ	0.0	-0.045790
δ	2.0	1.960979
b_5	2.0	2.07192
t_2	100.0	100.0
$tp\ (x, y)$	(50.0, 2.0)	(51.34, 0.721)

13. **Case (m)**

Figure 5.14 presents the result obtained using the proposed calibration mechanism. It can be seen from the figure that even though there exists reasonable difference between the initial and observed path, after calibration the calibrated path is very close to the observed path. Table 5.13 presents the initial and calibrated values of the parameters of the potential field theory model.

Table 5.13: Initial and calibrated parameter values for Case (m)

Parameters of the potential functions	**Parameters values**	
	Initially assumed	**After calibration**
a_1	1.0	2.8499
b_1	0.32641	0.806805
a_2	4.0	3.45001
b_2	0.04663	0.121544
a_4	2.0	3.420
m_a	8.0	9.2100
b_4	2.0	1.57306
t_1	0.0	0.0
α	0.0	0.0
β	0.0	0.000216
γ	0.0	-0.024475
δ	2.0	1.57306
b_5	2.0	1.56986
t_2	100.0	100.0
$tp\ (x, y)$	(50.0, 2.3)	(51.43, 0.923)

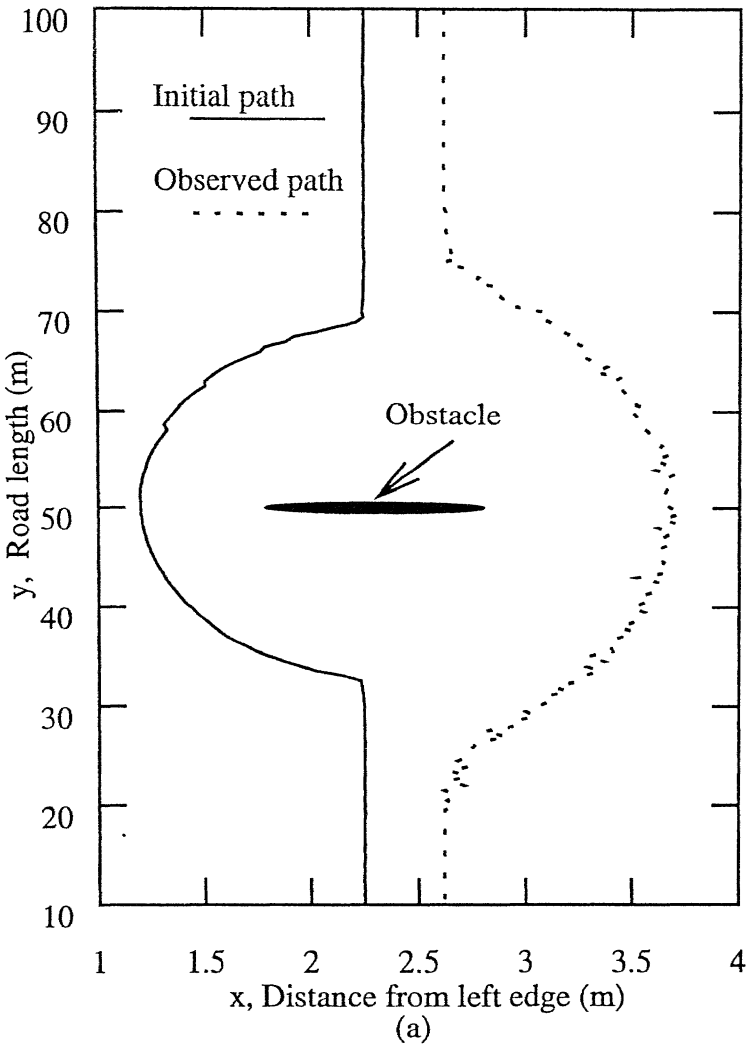

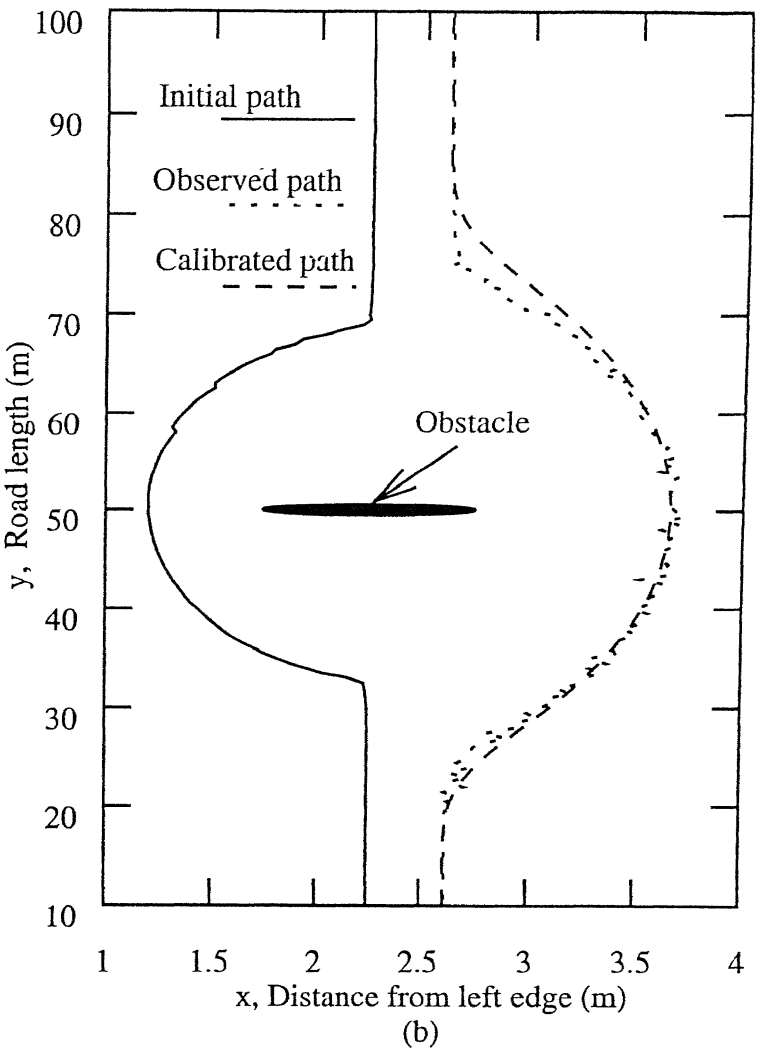

Figure 5.14: Result showing (a) the initial and observed paths and (b) the initial, observed and calibrated paths for Case (m)

Chapter 6

CONCLUSIONS

In this thesis a calibration mechanism which can calibrate the parameter values of potential field function of road edges and static obstacles is developed. In order to developed this mechanism a detail parametric study of potential field function is under taken and completed. Results showing the efficacy of proposed mechanism in calibrating the parameters are also presented.

Although the proposed mechanism can ably calibrate the parameters it is felt that the efficiency of the algorithm can be further improved. For example, currently the step side for the corrections have been kept small. Although a attempt has been made to determine which parameter in which situation should be changed in larger step sizes, the determination is largely ad hoc. It is felt that a detail study on the step size should be conducted so that the calibrated values can be obtained faster.

Another short coming of this thesis is that the observed paths were generated rather than experimentally obtained. Although it is felt that the proposed calibration algorithm will function equally well even if observed paths are experimentally obtained one can never be cent percent confident.

It also felt the scope of this study should be enlarged to cover dynamic obstacles like moving vehicles. further, no attempt was made to calibrate the parameters of the models developed by Vasishta [2] and Agrawal [1] only the parameters of the potential functions were calibrated. This shortcoming must also be looked into. Also, the calibration was done based only on the observed position profile (i.e., the observed path of the driver) and did not use information on the velocity

profile (i.e., observed velocities of driver). This drawback needs to be rectified.

Finally a study should be conducted to see whether the calibrated potential field function can predict the driver path reasonably well for driving scenarios which are not used in the calibration process. This test is imperative to see whether the calibration process makes meaningful changes to the potential field functions.

References

[1] Saurabh Kumar Agrawal. Modelling of Driver Behavior in the presence of other moving vehicles, *M.Tech Thesis*, Indian Institute of Technology, Kanpur, October 2000.

[2] Kyatham Vasishta. Preliminary Explorations into Modelling of Driver Behaviour, *M.Tech Thesis*, Indian Institute of Technology, Kanpur, July 1999.

[3] J.C. Latombe. *Robot Motion Planning.* Kluwer Academic Publishers, Boston, 1991.

[4] Louis A. Pipes. Car Following Models and Fundamental Diagram of Road Traffic. *Transportation Research*, Vol. 1, 1967, pp. 21-29.

[5] T. W. Forbes, H. J. Zagorski, E. L. Holshouser, and W. A. Deterline. Measurement of Driver Reactions to Tunnel conditions. *Highway Research Board Proceedings*, Vol. 37, 1958, pp. 60-66.

[6] T. W. Forbes. Human Factor Considerations in Traffic Flow Theory. *Highway Research Record*, No. 15, 1963, pp. 60-66.

[7] Robert E. Chandler, Robert Herman, and Elliott W. Montroll. Traffic Dynamics: Studies in Car Following. *Operations Research*, Vol. 6, No. 2, 1958, pp. 165-184.

[8] Robert Herman, Elliott W. Montroll, Renfry B. Potts, Richard W. Rothery. Traffic Dynamics: Analysis of Stability in Car Following. *Operations Research*, Vol. 7, No. 1, 1959, pp. 86-106.

[9] Robert Herman and Renfrey B. Potts. Single Lane Traffic Theory and Experiment. *Proceedings of the Symposium on the Theory of Traffic Flow*, 1959, pp. 120-146.

[10] Denos C. Gazis, Robert Herman, and Renfry B. Potts. Car Following Theory of Steady State Flow. *Operations Research*, Vol. 7, No. 4, 1959, pp. 499-505.

[11] Denos C. Gazis, Robert Herman, and Richard W. Rothery. Nonlinear Follow-the-Leader Models of Traffic Flow. *Operations Research*, Vol. 9, No. 4, 1961, pp. 545-567.

[12] Thomas H. Rockwell, Ronal L. Ernest, and Albert Hanken. A Sensitivity Analysis of Empirically Derived Car-following Models. *Transportation Research*, Vol. 2, 1968, pp. 363-373.

[13] Adolf D. May and Hartmut E. M. Keller. Non-Integer Car-Following Models. *Highway Research Record*, No. 199, 1967, pp. 19-32.

[14] S. Kikuchi. and P. Chakroborty Car-Following Model Based on Fuzzy Inference System, *Transportation Research Record-1365*, TRB, National Research Council, Washington. D. C., 1992, pp. 82-91.

[15] Partha Chakroborty and Shinya Kikuchi. Evaluation of the General Motors Based Car-Following Models and a Proposed Fuzzy Inference Model, *Transportation Research Part C*, Vol. 7, 1999, pp. 209-235.

[16] A. Taragin. Driver Behavior as Affected by Objects on Highway Shoulders, *Highway Research Board Proceedings*, Vol. 34, 1955, pp. 453-472.

[17] R. M. Michaels and L. W. Gozan. Perceptual and Field Factors Causing Lateral Displacement, *Highway Research Record*, No. 25, Highway Research Board, National Research Council, Washington, D.C., 1963.